Morita et al. Reproductive Biology and Endocrinology 2012, 10:14
http://www.rbej.com/content/10/1/14

REPRODUCTIVE BIOLOGY AND ENDOCRINOLOGY

RESEARCH Open Access

Resveratrol promotes expression of SIRT1 and StAR in rat ovarian granulosa cells: an implicative role of SIRT1 in the ovary

Yoshihiro Morita[1], Osamu Wada-Hiraike[1*], Tetsu Yano[1], Akira Shirane[1], Mana Hirano[1], Haruko Hiraike[1], Satoshi Koyama[1], Hajime Oishi[1], Osamu Yoshino[1], Yuichiro Miyamoto[1], Kenbun Sone[1], Katsutoshi Oda[1], Shunsuke Nakagawa[2], Kazuyoshi Tsutsui[3] and Yuji Taketani[1]

Abstract

Background: Resveratrol is a natural polyphenolic compound known for its beneficial effects on energy homeostasis, and it also has multiple properties, including anti-oxidant, anti-inflammatory, and anti-tumor activities. Recently, silent information regulator genes (Sirtuins) have been identified as targets of resveratrol. Sirtuin 1 (SIRT1), originally found as an NAD^+-dependent histone deacetylase, is a principal modulator of pathways downstream of calorie restriction, and the activation of SIRT1 ameliorates glucose homeostasis and insulin sensitivity. To date, the presence and physiological role of SIRT1 in the ovary are not known. Here we found that SIRT1 was localized in granulosa cells of the human ovary.

Methods: The physiological roles of resveratrol and SIRT1 in the ovary were analyzed. Immunohistochemistry was performed to localize the SIRT1 expression. SIRT1 protein expression of cultured cells and luteinized human granulosa cells was investigated by Western blot. Rat granulosa cells were obtained from diethylstilbestrol treated rats. The cells were treated with increasing doses of resveratrol, and subsequently harvested to determine mRNA levels and protein levels. Cell viability was tested by MTS assay. Cellular apoptosis was analyzed by caspase 3/7 activity test and Hoechst 33342 staining.

Results: SIRT1 protein was expressed in the human ovarian tissues and human luteinized granulosa cells. We demonstrated that resveratrol exhibited a potent concentration-dependent inhibition of rat granulosa cells viability. However, resveratrol-induced inhibition of rat granulosa cells viability is independent of apoptosis signal. Resveratrol increased mRNA levels of SIRT1, LH receptor, StAR, and P450 aromatase, while mRNA levels of FSH receptor remained unchanged. Western blot analysis was consistent with the results of quantitative real-time RT-PCR assay. In addition, progesterone secretion was induced by the treatment of resveratrol.

Conclusions: These results suggest a novel mechanism that resveratrol could enhance progesterone secretion and expression of luteinization-related genes in the ovary, and thus provide important implications to understand the mechanism of luteal phase deficiency.

Keywords: SIRT1, Resveratrol, Ovary, Granulosa cells, Luteinization

* Correspondence: osamu.hiraike@gmail.com
[1]Department of Obstetrics and Gynecology, Graduate School of Medicine, The University of Tokyo, 7-3-1, Hongo, Bunkyo-ku, Tokyo 113-8655, Japan
Full list of author information is available at the end of the article

Background

The study of natural compounds with pharmacological activity has become an emerging trend in nutritional and pharmacologic research. Polyphenols represent a vast group of compounds having aromatic ring, characterized by the presence of one or more hydroxyl groups with various structural complexities. Resveratrol (trans-3, 5, 40-trihydroxystilbene) is a natural polyphenol synthesized by plants as a phytoalexin that becomes activated under stress conditions such as ultraviolet radiation and fungal infection [1,2]. It can be found in berries, nuts and some medicinal plants, and mainly present in the skin of grapes and thus in red wine [3]. Previous studies have reported its anti-oxidant, anti-inflammatory, and growth-inhibitory activities using several cancer cell lines and animal models [2,4,5]. These properties of resveratrol have been linked to the inhibition of proliferation in association with cell cycle arrest and apoptotic cell death typically observed in vitro at concentrations in the range of 10-300 μM [5-7]. Thus, resveratrol has activity in regulating multiple cellular events associated with carcinogenesis, and the activation of SIRT1 is postulated to be a key event to elucidate the pathophysiology of resveratrol [8,9]. SIRT1, the mammalian homologue of yeast Sir2 (silent information regulator 2), functions as an NAD $^{+}$-dependent class III histone deacetylase. SIRT1 deacetylates multiple targets in mammalian cells, including p53, FOXO1, FOXO3, PGC-1α, liver X receptor, NBS1 and hypoxia-inducible factor 2α [10,11]. By regulating these molecules, SIRT1 functions as a master regulator of energy homeostasis, gene silencing, metabolism, genomic stability, and cell survival.

The ability of the ovary to produce growing follicles that ovulate is the basis of female fertilization. A critical feature of ovarian granulosa cell (GC) function is the differentiation of the ovulatory follicle into the corpus luteum which mainly produces progesterone (P4) that is important for the maintenance of pregnancy. Recently, it has been suggested that SIRT1 activator resveratrol plays a role in reproductive biology. Resveratrol was shown to modulate theca cell proliferation [12], and methylated resveratrol analogues possessed biological activities in swine GCs [13]. In the present study, to assess a role of SIRT1 in the regulation of reproductive axis in female, we investigated the expression of endogenous SIRT1 in human and rat GCs and the effect of resveratrol on cellular viability and steroidogenesis in rat GCs.

Methods

Chemicals

Diethylstilbestrol (DES) and resveratrol were purchased from Sigma-Aldrich (St. Louis, MO, USA). All other chemicals, unless otherwise mentioned, were obtained from Sigma-Aldrich.

Human cancer cell lines and primary human GCs

Human cervical cancer cell line HeLa was purchased from American Type Culture Collection (Manassas, VA, USA). Human ovarian granulosa-like tumor cell line KGN, which originated from a Stage III granulosa cell carcinoma in a 63-year-old Japanese women [14], was obtained from RIKEN Cell Bank of Japan (Tsukuba, Japan). Primary human GCs were obtained from patients undergoing transvaginal oocyte retrieval for in vitro fertilization at the University of Tokyo Hospital. The method to purify human GCs was described previously [15]. The study was approved by the Institutional Review Board of the University of Tokyo, and written informed consent for the research use of human GCs was obtained from each patient. These cells were maintained in Dulbecco's modified Eagle Medium (DMEM)/F12 medium (Invitrogen, Carlsbad, CA, USA) supplemented with 10% charcoal-stripped fetal bovine serum (FBS; Invitrogen), 100 U/ml penicillin, 100 μg/ml streptomycin and 0.25 μg/ml amphotericin B in a humidified atmosphere of 5% CO_2 and 95% air at 37°C.

Preparation and culture of rat GCs

Guidelines for the care and use of laboratory animals as adopted and promulgated by the University of Tokyo were followed. Twenty-three-day-old immature female Wistar rats were purchased from CLEA Japan, Inc. (Tokyo, Japan) and housed in a temperature-controlled room with a 12 h light/12 h dark schedule. Pelleted food and water were provided ad libitum. Rats were implanted with SILASTIC capsules (Dow Corning, Corp., Midland, MI, USA) containing 10 mg DES to increase GC number [16], and killed 4 days later by cervical dislocation. Removed ovaries were immediately cleaned of surrounding connective tissues and placed into DMEM/F12 medium supplemented with 10% charcoal-stripped FBS, 100 U/ml penicillin, 100 μg/ml streptomycin and 0.25 μg/ml amphotericin B. GCs were harvested by needle puncture of ovarian follicles, suspended in the medium, and purified by filtration with a 100-μm cell strainer and then a 40-μm cell strainer (BD Biosciences, Bedford, MA, USA). Isolated GCs were washed twice by centrifugation at 200 × g for 5 min and cultured in the medium in a humidified atmosphere of 5% CO_2 and 95% air at 37°C [17].

Tissue samples and immunohistochemistry

The ovarian tissues used in this study were obtained from 5 female patients with regular menstrual cycles who were taking no hormonal drugs and underwent

radical or extended hysterectomy for carcinoma of the uterine cervix and endometrium. The female patients were 32-44 years old at the time of operation and the operations were performed in proliferative phase of the menstrual cycle. The study was approved by the Institutional Review Board of the University of Tokyo, and written informed consent was obtained in each instance. Immunohistochemistry was performed as described previously [18]. Paraffin sections (4 μm) were dewaxed in xylene and rehydrated through graded ethanol to water. Antigens were retrieved by boiling in 10 mM citrate buffer (pH 6.0) for 30 min. The cooled sections were incubated in DAKO REAL Peroxidase-Blocking solution (DAKO, Carpinteria, CA, USA) for 30 min to quench endogenous peroxidase. To block the nonspecific binding, sections were incubated in PBS containing 3% BSA and 0.5% Nonidet P-40 for 10 min at room temperature. Sections were then incubated with the rabbit polyclonal antibody to SIRT1 (sc-15404, Santa Cruz Biotechnology, Inc., Santa Cruz, CA, USA) in DAKO REAL Antibody Diluent (DAKO) overnight at 4°C. Negative controls were incubated with preimmune serum IgG fraction. ChemMate EnVision Detection system (DAKO) was used to visualize the signal. The sections were developed with 3,3'-diaminobenzidine tetrahydrochloride substrate (DAKO), lightly counterstained with ae's hematoxylin (Wako Chemical, Tokyo, Japan), dehydrated through ethanol series and xylene, and mounted.

Western blotting

HeLa cells, KGN cells, and human GCs were seeded into 6-cm culture dishes (BD Biosciences) at a density of 1×10^6 cells/dish in 3 ml of the culture medium. After 48 h, the cells were harvested with trypsin (0.05%)/EDTA (0.02%) and scraped into the lysis buffer containing 50 mM Tris-HCl (pH 8.0), 150 mM NaCl, 0.02% sodium azide, 0.1% sodium dodecyl sulfate, 1% Nonidet P-40, and 0.5% sodium deoxycholate for 30 min on ice. Rat GCs were seeded into 10-cm culture dishes (BD Biosciences) at a density of 2-3 × 10^6 cells/dish in 10 ml of the culture medium. After 48 h, the medium was replaced with fresh medium containing 1% charcoal-stripped FBS and 100 μM of resveratrol, and cell culture was continued. Thereafter GCs were harvested, and lysed. Insoluble material was removed by centrifugation at 12,000 × g, for 20 min at 4°C. The supernatants were recovered, and the protein concentrations were measured using Bio-Rad protein assay reagent (Bio-Rad Lab., Hercules, CA, USA). Equivalent amounts of lysate protein (30 μg were subjected to 10% SDS-PAGE and electrophoretically transferred onto polyvinylidene difluoride membranes (Millipore Corp., Billerica, MA, USA). After blocking nonspecific binding sites by incubation for 1 h with Tris-buffered saline (25 mM Tris and 150 mM NaCl, pH 7.6) containing 5% nonfat milk and 0.2% Tween 20, the membranes were blotted with the primary antibodies overnight at 4°C. The primary antibodies used were anti-DBC1 [19] and anti-P450 aromatase (P450arom; MCA2077S, AbD serotec, Oxford, UK). Anti-SIRT1 (sc-15404), anti-StAR (sc-25806), and anti-LH receptor (LH-R; sc-25828) were purchased from Santa Cruz Biotechnology Inc. (Santa Cruz). Reactive proteins were detected with horseradish peroxidase-conjugated secondary antibodies (Cell Signaling Technology, Inc., Beverly, MA, USA) for 60 min at room temperature and developed with ECL Plus western blotting detection reagents (GE Healthcare, Little Chalfont, UK). The membranes were stripped with the buffer containing 100 mM 2-mercaptoethanol, 2% SDS and 62.5 mM Tris- HCl (pH 6.7), then reprobed with mouse monoclonal antibody to β-Actin (sc-47778, Santa Cruz Biotechnology, Inc.) to confirm equivalent protein loading. The images were scanned by the luminescent image analyzer Image Quant LAS 4000 mini (GE Healthcare).

Granulosa cell progesterone production

Culture media for the Western blot were collected, frozen, and stored at -20°C until P4 determination by Progesterone EIA kit (Cayman Chemical Co., Ann Arbor, MI, USA). P4 assay was performed according to the manufacture's instruction. The data are expressed as the amount of steroids (pg/ml) secreted. The results are representative of three to four independent cultures with each condition in quadruplet.

Cell viability assay

Viability of rat GCs was examined by using the 3-(4,5-dimethylthiazol-2-yl)-5- (3-carboxymethoxyphenyl)-2-(4-sulfophenyl)-2H-tetrazolium, inner salt (MTS) assay kit (CellTiter 96 Aqueous One Solution Cell Proliferation Assay; Promega, Madison, WI, USA) according to the manufacturer's instructions. Briefly, cells were seeded into 96-well plates (BD Biosciences) at a density of 1 × 10^4 cells/well in 100 μL of the culture medium. After 48 h, the medium was replaced with fresh medium containing 1% charcoal-stripped FBS and various concentrations of resveratrol, and cell culture was continued for a further 72 h. Resveratrol was dissolved in dimethyl sulfoxide and diluted with the medium to yield desired concentrations. The final concentration of dimethyl sulfoxide never exceeded 0.05%. The effects of resveratrol were investigated at concentrations between 10 and 100 μM in consideration of those used in the other studies where resveratrol inhibited the proliferation of various cell types at concentrations in the range of 10-300 μM [5-7]. Finally, the medium was replaced with 100 μL of fresh medium containing 20 μL of MTS solution and incubated for an additional 4 h. Mitochondrial

dehydrogenase enzymes of viable cells converted MTS tetrazolium into a colored formazan product. The optical density of samples was read at 490 nm in the spectrophotometric microplate reader (BioTek, Winooski, VT, USA).

Reverse transcription and quantitative real-time PCR

Rat GCs were seeded into 6-cm culture dishes (BD Biosciences) at a density of 1×10^6 cells/dish in 3 ml of the culture medium. After 48 h, the medium was replaced with fresh medium containing 1% charcoal-stripped FBS and various concentrations of resveratrol (10-100 μM, and cell culture was continued for a further 24 h. Total cellular RNA was extracted using RNeasy Mini Kit (Qiagen, Hilden, Germany) and quantified by measuring absorbance at 260 nm and stored at -80° until assay. The mRNA levels of relevant molecules were measured by quantitative real-time RT-PCR using One Step SYBR PrimeScript RT-PCR Kit (TaKaRa Bio. Inc., Tokyo, Japan) in the Light Cycler (Roche Applied Science, Mannheim, Germany). Accumulated levels of fluorescence were analyzed by the second-derivative method after the melting-curve analysis, and then the expression levels of target genes were normalized to the expression level of β-Actin in each sample. Primer pairs of analyzed mRNA are described in Table 1.

Table 1 Primer sequences used for quantitative real-time PCR

Gene	Primers	Primer Sequence	Expected size in base pair
β-actin	Sense	CGAGTACAACCTTCTTGCAG	207
	Antisense	TTCTGACCCATACCCACCAT	
Bax	Sense	GAATTGGCGATGAACTGGAC	157
	Antisense	GCAAAGTAGAAAAGGGCAACC	
Bcl2	Sense	AACATCGCTCTGTGGATGAC	150
	Antisense	GAGCAGCGTCTTCAGAGACA	
DBC1	Sense	TCTCCAAGTCTCGCCTGTG	158
	Antisense	CTCTGTTGCCTCCAACCAGT	
FSH-R	Sense	ATGGCCCCCATTTCATTCTT	82
	Antisense	ACTAGGAGAATCTTGGCCTTGGA	
LH-R	Sense	ATTGACACTCTGCTTAACTTTCCATCT	82
	Antisense	TGGCCATGAGGTACTCATGATCT	
p450arom	Sense	TCCTCAGCAGAGAAACTGGAAGA	151
	Antisense	CGTACAGAGTGACGGACATGGT	
SIRT1	Sense	TGTTTCCTGTGGGATACCTGA	137
	Antisense	TGAAGAATGGTCTTGGGTCTTT	
StAR	Sense	AGGAAAACAGAACTGAGGCTTAGAATA	93
	Antisense	AAGGTTTCATAGATACCTGTCCCTTAAC	

Caspase-3/7 activity assay

Apoptosis executioner caspase-3/7 activity in rat GCs was measured using the Apo-ONE Homogeneous Caspase-3/7 Assay kit (Promega) according to the manufacturer's instructions. Briefly, cells were seeded into 96-well plates (BD Biosciences) at a density of 1×10^4 cells/well in 100 μL of the culture medium. After 48 h, the medium was replaced with fresh medium containing 1% charcoal-stripped FBS and various concentrations of resveratrol (10- 100 μM), and cell culture was continued for 6, 12 and 24 h. Caspase-3/7 activity was measured at excitation wavelength 485 nm and emission wavelength 528 nm in the spectrophotometric microplate reader (BioTek).

Hoechst 33342 nuclear staining

Hoechst staining was performed to confirm the apoptotic profile as a result of morphological change in the nucleus in which Hoechst 33342 binds specifically to A-T base region in DNA and emits fluorescence. Rat GCs were seeded into 8-well chamber slides (Nalge Nunc International, Naperville, IL, USA) at a density of 1×10^5 cells/well in 400 μl of the culture medium. After 48 h, the medium was replaced with fresh medium containing 1% charcoal-stripped FBS and resveratrol (50 and 100 μM), and cell culture was continued for 6, 12, 24 and 48 h. Finally, cells were rinsed in PBS and fixed with 4% paraformaldehyde in PBS (pH 7.4) at room temperature for 30 min. Then cells were rinsed in PBS twice and stained with Hoechst 33342 (10 μg/ml in PBS) for 3 min. The specimens were mounted with Vectashield medium (Vector Labs. Inc., Burlingame, CA, USA) and photographs were taken at X200 magnification under a fluorescent confocal microscope (Carl-Zeiss MicroImaging Inc., Oberkochen, Germany).

Statistical analysis

Data represent the mean ± SEM from at least three independent experiments. Statistical analyses were carried out by one-way ANOVA with *post-hoc* test for multiple comparisons by using StatView software (SAS Institute Inc., Cary, NC, USA). $P < 0.05$ was considered statistically significant.

Results

Expression of SIRT1 protein in human GCs

We investigated the localization of SIRT1 protein in the human ovary using immunohistochemistry. Expression of SIRT1 was observed in nuclei of GCs at various stages of follicular development (Figure 1A-C). Part of the theca interstitial cells and the oocyte were also found to have positive signals. To confirm the expression of SIRT1, luteinized human granulosa cells were obtained from women undergoing in vitro fertilization

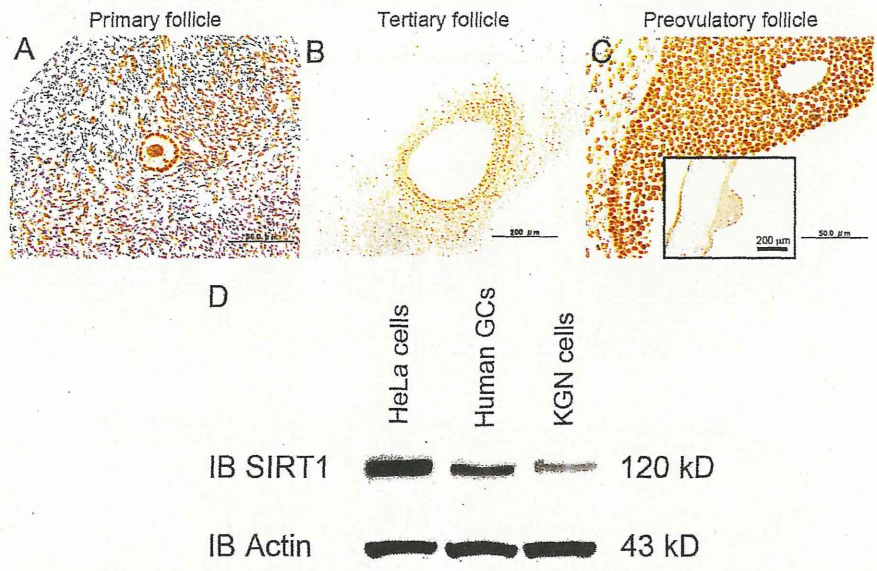

Figure 1 Expression of SIRT1 protein in human GCs. Immunohistochemical detection of SIRT1 in the human ovary (A, primary follicle; B, tertiary follicle; C, preovulatory follicle). Representative data from five specimens were shown. Nuclei of GCs were positively stained with anti-SIRT1 antibody at various stages of follicular development. Bars indicate (A) 50 μm, (B) 200 μm, and (C) 50 μm in high-power field and 200 μm in low-power field. SIRT1 was detected in primary (A), tertiary (B), and preovulatory (C) follicles of granulosa cells. Note that a part of the theca cells and oocyte nucleus are stained. Negative controls included a section incubated with preimmune rabbit IgG. (D) Western blotting revealed the presence of SIRT1 in KGN cells, human GCs, and HeLa cells (positive control).

program, and Western blot analysis revealed the expression of SIRT1 protein in KGN cells and human GCs (Figure 1D). HeLa cells were used as a positive control for Western blot because we [19] and other investigators [20] have detected the expression of SIRT1 protein.

Effect of resveratrol on cell viability and expression of SIRT1 and DBC1 in cultured rat GCs

To determine whether activation of SIRT1 by resveratrol affects rat GC viability, the extent of cell viability was measured by MTS assay. Resveratrol, at concentrations between 50 and 100 μM, produced a dose-dependent inhibition of cell viability after 72 h of treatment, with the maximal effect (reduction to 22.8 ± 4.4% of the control) being observed at 100 μM (Figure 2A). Recent studies have shown that DBC1 promotes p53-mediated apoptosis through specific inhibition of deacetylase activity of SIRT1 [21,22]. To determine whether the inhibitory effect on cell viability by resveratrol is related to the change in SIRT1 activation, the effect of resveratrol on mRNA levels of SIRT1 and DBC1, a negative regulator of SIRT1, was investigated by quantitative real-time RT-PCR in cultured rat GCs. After 24 h culture of rat GCs, mRNA levels of SIRT1 significantly increased at 100 μM (Figure 2B), while those of DBC1 remained unchanged (Figure 2C). Western blot analysis was also performed to confirm the result of quantitative real time RT-PCR and resveratrol-dependent induction of SIRT1 protein was observed (Figure 2D)

Effect of resveratrol on cell-death machinery in cultured rat GCs

Resveratrol has been shown to induce cell-cycle arrest and apoptosis in various cell lines [5,12]. To determine whether the reduction of the viability of rat GCs by resveratrol is due to the induction of apoptosis, the effect of resveratrol on mRNA levels of the representative apoptosis promoter Bax and inhibitor Bcl-2 was analyzed by quantitative real-time RT-PCR in cultured rat GCs at concentrations of resveratrol between 10 and 100 μM. The significant change in mRNA levels of Bax and Bcl-2 was not found at 24 h (Figure 3A, B). Apoptosis executioner caspase-3/7 activity was measured in cultured rat GCs at concentrations of resveratrol ranging from 10 to 100 μM and at various time points (6, 12, and 24 h). Resveratrol significantly inhibited caspase-3/7 activity at 75 and 100 μM after 24 h of treatment (Figure 3C). Furthermore, the effect of resveratrol on the incidence of apoptotic cells was investigated by Hoechst 33342 nuclear staining. Resveratrol (50 and 100 μM) showed no typical apoptotic changes including nuclear shrinkage, chromatin condensation, and nuclear fragmentation in cultured rat GCs at 6, 12, 24, and 48 h (Figure 3D).

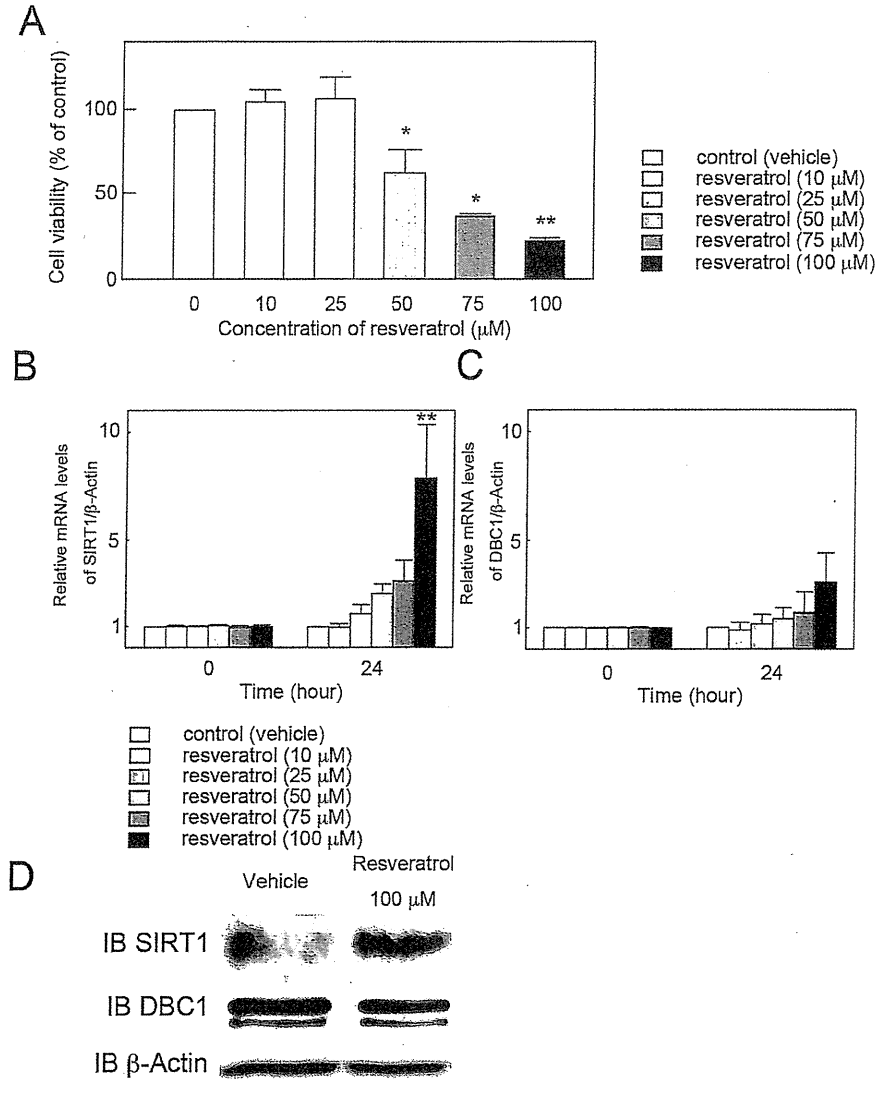

Figure 2 Effect of resveratrol on cell viability and expression of SIRT1 and DBC1 in cultured rat GCs. (A) Effect of resveratrol on cell viability at 72 h was estimated by MTS assay. Results are shown as the mean percentage of the untreated control ± SEM (bars) of eight wells of three independent experiments * $p < 0.05$ *vs.* control. ** $p < 0.01$ *vs.* control. (B and C) Effect of resveratrol on mRNA levels of (B) SIRT1 and (C) DBC1 was investigated by quantitative real-time RT-PCR. The mRNA level of the untreated control was arbitrarily set at 1.0, and that of the treatment group was estimated relative to the control value. Results are shown as the mean ± SEM (bars) of three independent experiments. ** $p < 0.01$ *vs.* control. (D) Effect of resveratrol on protein levels of SIRT1 was investigated by Western blot. Resveratrol treatment resulted in an increased expression of SIRT1 protein, and the results were consistent with that of quantitative real time RT-PCR. Three independent experiments were performed and a representative result is shown.

Effect of resveratrol on folliculogenesis-related molecules in cultured rat GCs

The Effect of resveratrol on mRNA levels of folliculogenesis-related molecules was investigated by quantitative real-time RT-PCR in cultured rat GCs at concentrations of resveratrol between 10 and 100 μM. After 24 h culture, resveratrol significantly increased mRNA levels of LH-R, steroidogenic acute regulatory protein (StAR), and P450arom at 100 μM (Figure 4B-D), while FSH receptor (FSH-R) mRNA levels remained unchanged (Figure 4A). Western blot analysis was also performed to confirm the result of quantitative real time RT-PCR and resveratrol-dependent stimulation of StAR, LH-R, and P450arom protein was confirmed (Figure 4E). To investigate the possibility that resveratrol promote steroidgenesis, serum concentration of P4 was evaluated and it has been revealed that resveratrol exhibited 3-fold enhancement of hormonal secretion at 48 h of culture (Figure 4F).

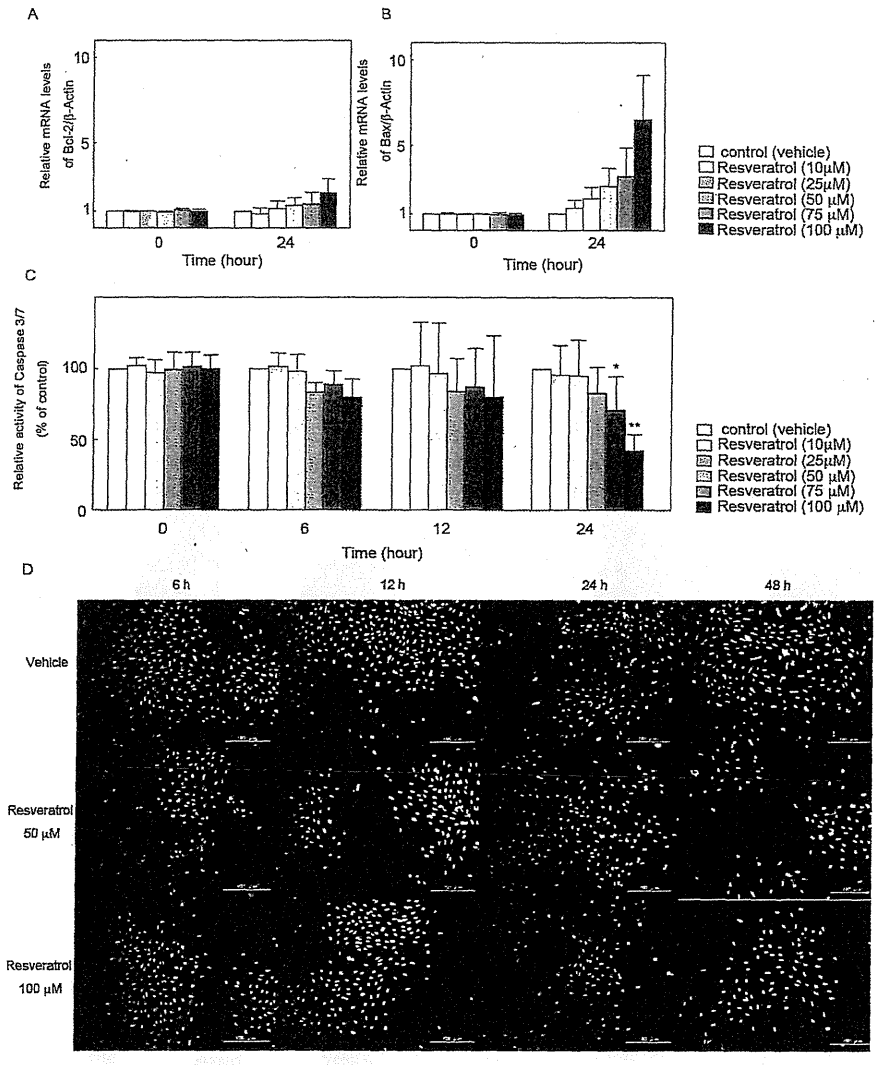

Figure 3 Effect of resveratrol on cell-death machinery in cultured rat GCs. Effect of resveratrol on mRNA levels of (A) Bcl-2 and (B) Bax was investigated by quantitative real-time RT-PCR. The mRNA level of the untreated control was arbitrarily set at 1.0, and that of the treatment group was estimated relative to the control value. Results are shown as the mean ± SEM (bars) of three independent experiments. (C) Caspase-3/7 activity was measured by the Apo-ONE Homogeneous Caspase-3/7 Assay kit at 6, 12 and 24 h. Results are shown as the mean percentage of the untreated control ± SEM (bars) of eight wells of three independent experiments. (D) Hoechst 33342 staining of resveratrol-treated rat GCs at 6, 12, 24, and 48 h. * $p < 0.05$ *vs.* control. ** $p < 0.01$ *vs.* control.

Discussion

Recently, resveratrol has been the focus of many *in vitro* and *in vivo* studies because of its pleiotropic biological activities [1-9]. However, the studies of resveratrol in ovarian physiology are limited. Resveratrol has been reported to exert estrogenic effects, increasing uterine and ovarian wet weight [23]. It is a phytoestrogen known to bind equally to estrogen receptors α and β [24], and structurally similar to synthetic estrogens, such as DES and 17β-estradiol benzoate [25]. In contrast to its hyperproliferative effects, resveratrol promoted apoptosis in rat ovarian theca-interstitial cells [12], and its analogues inhibited swine GC growth [13]. It was also reported that resveratrol inhibited the proliferation of a wide variety of human cancer cell lines through the induction of S-phase cell cycle arrest and apoptosis [5]. In the present study, we demonstrated that resveratrol exerted a dose-dependent inhibition of cell viability on rat GCs. This effect appeared not to be due to the induction of apoptosis, which was different from the previous findings in rat ovarian theca-interstitial cells [12]. Then we studied whether this resveratrol-induced decrease of cellular viability may lead to the differentiation of GCs.

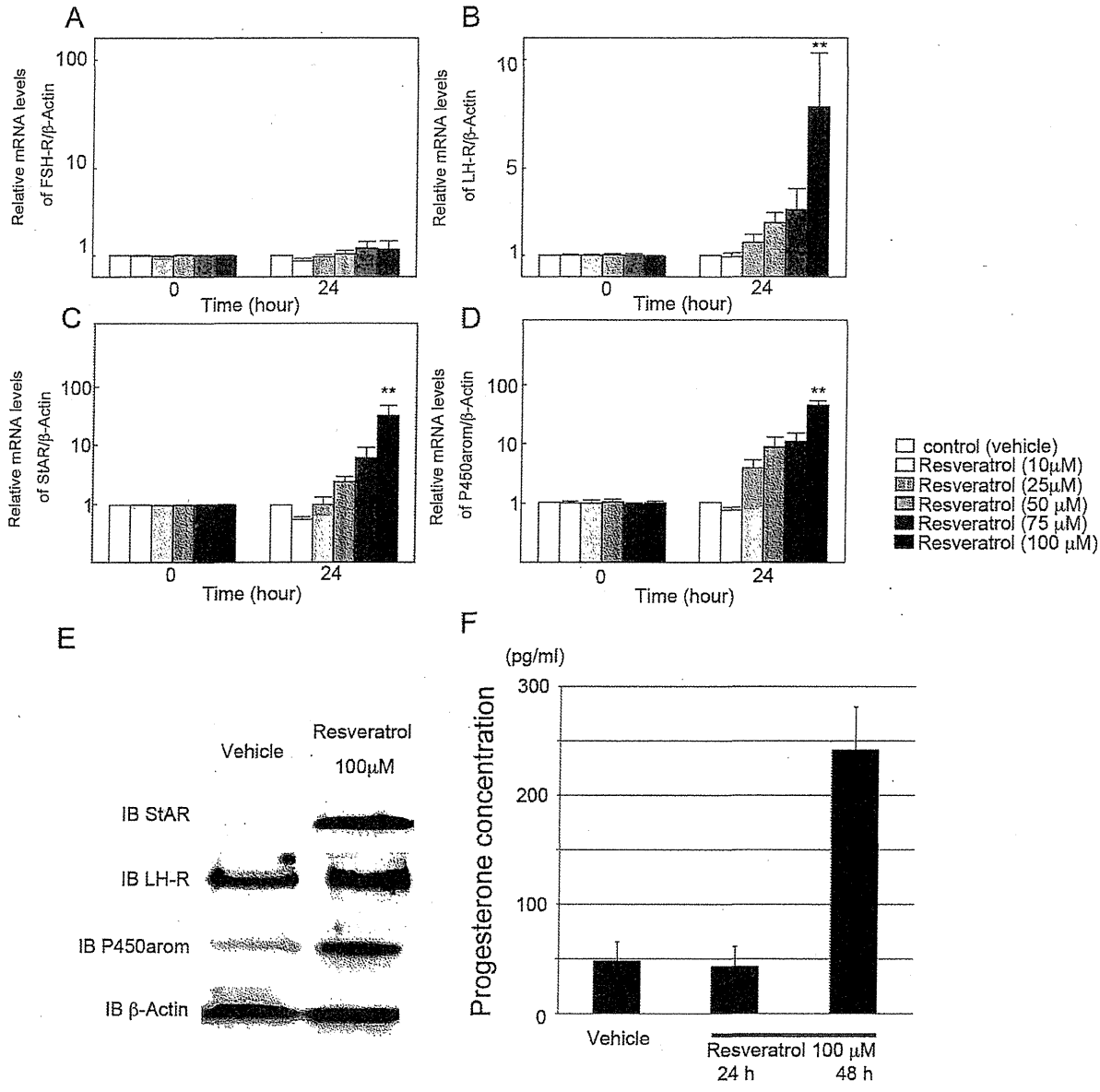

Figure 4 Effect of resveratrol on folliculogenesis-related molecules in cultured rat GCs. (A-D) Effect of resveratrol on mRNA levels of (A) FSH-R, (B) LH-R, (C) StAR and (D) P450arom was investigated by quantitative real-time RT-PCR. The mRNA level of the untreated control was arbitrarily set at 1.0, and that of the treatment group was estimated relative to the control value. Results are shown as the mean ± SEM (bars) of three independent experiments. ** $p < 0.01$ *vs.* control. (E) Effect of resveratrol on protein levels of StAR and P450arom was investigated by Western blot. Resveratrol treatment resulted in an increased expression of StAR, LH-R, and P450arom, and the results were consistent with those of quantitative real time RT-PCR. Three independent experiments were performed and a representative result is shown. (F) Effect of resveratrol on P4 secretion by rat granulosa cells. P4 secretion was measured by EIA protocol in culture medium of granulosa cells after 24 to 48 h of culture in DMEM/F-11 medium in the presence of resveratrol (100 μM). The data are expressed as the amount of steroids (pg/ml) secreted. The results, expressed as means ± SEM, are representative of three to four independent cultures with each condition in quadruplet.

Sirtuins are a conserved family of NAD^+-dependent class III histone deacetylases involved in a number of cellular processes including gene silencing at telomere and mating loci, DNA repair, recombination, and aging [8,10,11]. Recent studies have established that SIRT1 plays an important role in the regulation of cell fate and stress response in mammalian cells, and promotes cell survival by inhibiting apoptosis or cellular senescence induced by stresses including DNA damage [11]. Indeed, resveratrol administration and accompanying activation

of SIRT1 has improved health and survival of mice on a high-calorie diet by ameliorating insulin resistance [9]. Here we demonstrated the expression of SIRT1 in human GCs by immunohistochemical and Western blot analysis, and the expression of its mRNA in rat GCs by RT-PCR. To our knowledge, this is the first report that SIRT1 is expressed in the ovarian follicular cells. It is also interesting that resveratrol treatment caused an increase in SIRT1 mRNA levels as well as the stimulation of the deacetylating function of SIRT1. Similar to this result, the mouse experimental model of dextran sodium sulfate-induced colitis was associated with a decrease in SIRT1 gene expression and resveratrol treatment significantly reversed the expression of SIRT1 [26]. However, it should be noted that all actions of resveratrol are not related to the activation of SIRT1 because resveratrol is an indirect activator of SIRT1 and has been shown to activate the expression and activity of nicotinamide phosphoribosyltransferase and AMP-activated protein kinase (AMPK) [27-30].

In our study, resveratrol increased the expression of P450arom and luteinization-related molecules, such as LH-R and StAR, in rat GCs, suggesting a possibility that resveratrol may promote steroidogenesis and luteinization, a process of terminal differentiation of GCs, in the ovary. In fact, P4 secretion was increased after resveratrol treatment. These findings are consistent with the previous study using HL60 promyelocytic cell line [31]. Since mRNA levels of LH-R in the human corpus luteum were reported to be about 7 times higher than those in preovulatory follicles [32], LH-R has been thought to be a key factor in the ability of GC to undergo luteinization. In the human and other primates, StAR is also essential for the development and maintenance of the corpus luteum. StAR is known to govern the rate-limiting step in steroidogenesis, which is the translocation of cholesterol from the outer to the inner mitochondrial membrane [33]. The process of luteinization is associated with up-regulation of StAR in luteinized granulosa cells. Considering the fact that StAR is not highly expressed in GCs of preovulatory follicles [34], our data may implicate a role of SIRT1 and its activator in promoting luteinization of the ovary. Following ovulation, GCs undergo luteinization and form the corpus luteum which secretes P4. Secretion of P4 is indispensable to cause secretory transformation of the endometrium so that implantation can occur. Before the placenta takes over P4 production, P4 produced by the corpus luteum provides the necessary support to early pregnancy. A defect in the corpus luteum function is associated with implantation failure and miscarriage [35]. Here we showed a new insight that the resveratrol treatment may serve, at least in part, as luteal support. Physiological roles of resveratrol in the ovary should be further determined because another possible beneficial effect on ovarian physiology is reported. Resveratrol is known as a pure aryl hydrocarbon receptor antagonist with no agonistic activity. Polycyclic aromatic hydrocarbons are environmental toxicants found in cigarette smoke, and stimulate aryl hydrocarbon receptor. Polycyclic aromatic hydrocarbons have detrimental effect on ovarian reserve via inducing Harakiri, and resveratrol may exert its rescuing effect by inhibiting Harakiri expression [36]. However, in view of the significant difference in the ovarian physiology between humans and rodents, our data should be interpreted with caution and the present observations should be verified using human GCs.

Conclusions

We have demonstrated that resveratrol plays a key role in the activation of luteinization, the terminal differentiation of GCs, and exerts its effects by stimulating the expression of SIRT1, StAR, LH-R, and P450arom in GCs. As a result of these effects, we found that resveratrol promoted P4 secretion. These results suggest that the stimulation of SIRT1 by resveratrol would be potentially beneficial in the treatment of luteal phase deficiency. Several chemical compounds are known to affect the SIRT1 activities, and SIRT1 stimulators are currently extensively investigated for the treatment of diabetes. We hypothesize that these drugs might have a role in ovarian physiology by affecting SIRT1, but further studies are necessary to confirm the physiological implication of SIRT1 in the ovary.

Abbreviations

DES: Diethylstilbestrol; DMEM: Dulbecco's Modified Eagle Medium; FBS: Fetal bovine serum; FSH-R: Follicle stimulating hormone receptor; GC: Granulosa cell; LH-R: Luteinizing hormone receptor; P4: Progesterone; P450arom: P450 aromatase; RT-PCR: Reverse transcript-polymerase chain reaction; StAR: Steroidogenic acute regulatory protein.

Acknowledgements

This study was supported by Grant-in-Aid for Scientific Research from the Ministry of Education, Science and Culture, JMS Bayer Schering Pharma Grant, Kowa Life Science Foundation, and Kanzawa Medical Research Foundation, Japan.

Author details

[1]Department of Obstetrics and Gynecology, Graduate School of Medicine, The University of Tokyo, 7-3-1, Hongo, Bunkyo-ku, Tokyo 113-8655, Japan. [2]Department of Obstetrics and Gynecology, School of Medicine, Teikyo University, 2-11-1 Kaga, Itabashi-ku, Tokyo 173-8605, Japan. [3]Laboratory of Integrative Brain Sciences, Department of Biology, Waseda University, 2-2, Wakamatsuchou, Shinjuku-ku, Tokyo, 162-8480, Japan.

Authors' contributions

YM carried out all of the experiments. AS, MH, HH, YM, and KS participated in the immunohistochemistry, real time PCR, Western blot, and hormonal quantification. OY helped to collect and purify rat GCs. SK, MH, and HO helped to collect human luteinized GCs from follicular aspirates. OW-H has been involved in acquisition of data, drafting the manuscript, and revising it critically for important intellectual content. KO, SN, and TY have made

substantial contributions to conception and design, analysis and interpretation of data. KT and YT have given final approval of the version to be submitted. All authors read and approved the final manuscript.

Competing interests
The authors declare that they have no competing interests.

Received: 5 September 2011 Accepted: 23 February 2012
Published: 23 February 2012

References

1. Langcake P, Pryce RJ: A new class of phytoalexins from grapevines. *Experientia* 1977, 33(2):151-152.
2. Gusman J, Malonne H, Atassi G: A reappraisal of the potential chemopreventive and chemotherapeutic properties of resveratrol. *Carcinogenesis* 2001, 22(8):1111-1117.
3. Jang M, Cai L, Udeani GO, Slowing KV, Thomas CF, Beecher CW, Fong HH, Farnsworth NR, Kinghorn AD, Mehta RG, *et al*: Cancer chemopreventive activity of resveratrol, a natural product derived from grapes. *Science* 1997, 275(5297):218-220.
4. Manna SK, Mukhopadhyay A, Aggarwal BB: Resveratrol suppresses TNF-induced activation of nuclear transcription factors NF-kappa B, activator protein-1, and apoptosis: potential role of reactive oxygen intermediates and lipid peroxidation. *J Immunol* 2000; 164(12):6509-6519.
5. Joe AK, Liu H, Suzui M, Vural ME, Xiao D, Weinstein IB: Resveratrol induces growth inhibition, S-phase arrest, apoptosis, and changes in biomarker expression in several human cancer cell lines. *Clin Cancer Res* 2002, 8(3):893-903.
6. van Ginkel PR, Sareen D, Subramanian L, Walker Q, Darjatmoko SR, Lindstrom MJ, Kulkarni A, Albert DM, Polans AS: Resveratrol inhibits tumor growth of human neuroblastoma and mediates apoptosis by directly targeting mitochondria. *Clin Cancer Res* 2007, 13(17):5162-5169.
7. Issuree PD, Pushparaj PN, Pervaiz S, Melendez AJ: Resveratrol attenuates C5a-induced inflammatory responses in vitro and in vivo by inhibiting phospholipase D and sphingosine kinase activities. *FASEB J* 2009, 23(8):2412-2424.
8. Howitz KT, Bitterman KJ, Cohen HY, Lamming DW, Lavu S, Wood JG, Zipkin RE, Chung P, Kisielewski A, Zhang LL, *et al*: Small molecule activators of sirtuins extend Saccharomyces cerevisiae lifespan. *Nature* 2003, 425(6954):191-196.
9. Baur JA, Pearson KJ, Price NL, Jamieson HA, Lerin C, Kalra A, Prabhu VV, Allard JS, Lopez-Lluch G, Lewis K, *et al*: Resveratrol improves health and survival of mice on a high-calorie diet. *Nature* 2006, 444(7117):337-342.
10. Michan S, Sinclair D: Sirtuins in mammals: insights into their biological function. *Biochem J* 2007, 404(1):1-13.
11. Finkel T, Deng CX, Mostoslavsky R: Recent progress in the biology and physiology of sirtuins. *Nature* 2009, 460(7255):587-591.
12. Wong DH, Villanueva JA, Cress AB, Duleba AJ: Effects of resveratrol on proliferation and apoptosis in rat ovarian theca-interstitial cells. *Mol Hum Reprod* 2010, 16(4):251-259.
13. Basini G, Tringali C, Baioni L, Bussolati S, Spatafora C, Grasselli F: Biological effects on granulosa cells of hydroxylated and methylated resveratrol analogues. *Mol Nutr Food Res* 2010, 54(Suppl 2):S236-243.
14. Nishi Y, Yanase T, Mu Y, Oba K, Ichino I, Saito M, Nomura M, Mukasa C, Okabe T, Goto K, *et al*: Establishment and characterization of a steroidogenic human granulosa-like tumor cell line, KGN, that expresses functional follicle-stimulating hormone receptor. *Endocrinology* 2001, 142(1):437-445.
15. Shi J, Yoshino O, Osuga Y, Nishii O, Yano T, Taketani Y: Bone morphogenetic protein 7 (BMP-7) increases the expression of follicle-stimulating hormone (FSH) receptor in human granulosa cells. *Fertil Steril* 2010, 93(4):1273-1279.
16. Otsuka F, Moore RK, Wang X, Sharma S, Miyoshi T, Shimasaki S: Essential role of the oocyte in estrogen amplification of follicle-stimulating hormone signaling in granulosa cells. *Endocrinology* 2005, 146(8):3362-3367.
17. Chen Q, Yano T, Matsumi H, Osuga Y, Yano N, Xu J, Wada O, Koga K, Fujiwara T, Kugu K, *et al*: Cross-Talk between Fas/Fas ligand system and nitric oxide in the pathway subserving granulosa cell apoptosis: a possible regulatory mechanism for ovarian follicle atresia. *Endocrinology* 2005, 146(2):808-815.
18. Wada-Hiraike O, Hiraike H, Okinaga H, Imamov O, Barros RP, Morani A, Omoto Y, Warner M, Gustafsson JA: Role of estrogen receptor beta in uterine stroma and epithelium: Insights from estrogen receptor beta-/- mice. *Proc Natl Acad Sci USA* 2006, 103(48):18350-18355.
19. Hiraike H, Wada-Hiraike O, Nakagawa S, Koyama S, Miyamoto Y, Sone K, Tanikawa M, Tsuruga T, Nagasaka K, Matsumoto Y, *et al*: Identification of DBC1 as a transcriptional repressor for BRCA1. *Br J Cancer* 2010, 102(6):1061-1067.
20. Kim JE, Lou Z, Chen J: Interactions between DBC1 and SIRT 1 are deregulated in breast cancer cells. *Cell Cycle* 2009, 8(22):3784-3785.
21. Kim JE, Chen J, Lou Z: DBC1 is a negative regulator of SIRT1. *Nature* 2008, 451(7178):583-586.
22. Zhao W, Kruse JP, Tang Y, Jung SY, Qin J, Gu W: Negative regulation of the deacetylase SIRT1 by DBC1. *Nature* 2008, 451(7178):587-590.
23. Henry LA, Witt DM: Resveratrol: phytoestrogen effects on reproductive physiology and behavior in female rats. *Horm Behav* 2002, 41(2):220-228.
24. Bowers JL, Tyulmenkov VV, Jernigan SC, Klinge CM: Resveratrol acts as a mixed agonist/antagonist for estrogen receptors alpha and beta. *Endocrinology* 2000, 141(10):3657-3667.
25. Gehm BD, McAndrews JM, Chien PY, Jameson JL: Resveratrol, a polyphenolic compound found in grapes and wine, is an agonist for the estrogen receptor. *Proc Natl Acad Sci USA* 1997, 94(25):14138-14143.
26. Singh UP, Singh NP, Singh B, Hofseth LJ, Price RL, Nagarkatti M, Nagarkatti PS: Resveratrol (trans-3,5,4'-trihydroxystilbene) induces silent mating type information regulation-1 and down-regulates nuclear transcription factor-kappaB activation to abrogate dextran sulfate sodium-induced colitis. *J Pharmacol Exp Ther* 2010, 332(3):829-839.
27. Hou X, Xu S, Maitland-Toolan KA, Sato K, Jiang B, Ido Y, Lan F, Walsh K, Wierzbicki M, Verbeuren TJ, *et al*: SIRT1 regulates hepatocyte lipid metabolism through activating AMP-activated protein kinase. *J Biol Chem* 2008, 283(29):20015-20026.
28. Suchankova G, Nelson LE, Gerhart-Hines Z, Kelly M, Gauthier MS, Saha AK, Ido Y, Puigserver P, Ruderman NB: Concurrent regulation of AMP-activated protein kinase and SIRT1 in mammalian cells. *Biochem Biophys Res Commun* 2009, 378(4):836-841.
29. Um JH, Park SJ, Kang H, Yang S, Foretz M, McBurney MW, Kim MK, Viollet B, Chung JH: AMP-activated protein kinase-deficient mice are resistant to the metabolic effects of resveratrol. *Diabetes* 2010, 59(3):554-563.
30. Chung S, Yao H, Caito S, Hwang JW, Arunachalam G, Rahman I: Regulation of SIRT1 in cellular functions: role of polyphenols. *Arch Biochem Biophys* 2010, 501(1):79-90.
31. Ragione FD, Cucciolla V, Borriello A, Pietra VD, Racioppi L, Soldati G, Manna C, Galletti P, Zappia V: Resveratrol arrests the cell division cycle at S/G2 phase transition. *Biochem Biophys Res Commun* 1998, 250(1):53-58.
32. Minegishi T, Tano M, Abe Y, Nakamura K, Ibuki Y, Miyamoto K: Expression of luteinizing hormone/human chorionic gonadotrophin (LH/HCG) receptor mRNA in the human ovary. *Mol Hum Reprod* 1997, 3(2):101-107.
33. Devoto L, Kohen P, Vega M, Castro O, Gonzalez RR, Retamales I, Carvallo P, Christenson LK, Strauss JF: Control of human luteal steroidogenesis. *Mol Cell Endocrinol* 2002, 186(2):137-141.
34. Kiriakidou M, McAllister JM, Sugawara T, Strauss JF: Expression of steroidogenic acute regulatory protein (StAR) in the human ovary. *J Clin Endocrinol Metab* 1996, 81(11):4122-4128.
35. Devoto L, Kohen P, Munoz A, Strauss JF: Human corpus luteum physiology and the luteal-phase dysfunction associated with ovarian stimulation. *Reprod Biomed Online* 2009, 18(Suppl 2):19-24.
36. Jurisicova A, Taniuchi A, Li H, Shang Y, Antenos M, Detmar J, Xu J, Matikainen T, Benito Hernandez A, Nunez G, *et al*: Maternal exposure to polycyclic aromatic hydrocarbons diminishes murine ovarian reserve via induction of Harakiri. *J Clin Invest* 2007, 117(12):3971-3978.

doi:10.1186/1477-7827-10-14
Cite this article as: Morita *et al.*: Resveratrol promotes expression of SIRT1 and StAR in rat ovarian granulosa cells: an implicative role of SIRT1 in the ovary. *Reproductive Biology and Endocrinology* 2012 10:14.

British Journal of Cancer (2011) 104, 1349 – 1355

www.bjcancer.com

Multifunctional transcription factor TFII-I is an activator of BRCA1 function

M Tanikawa[1], O Wada-Hiraike[*,1], S Nakagawa[1], A Shirane[1], H Hiraike[1], S Koyama[1], Y Miyamoto[1], K Sone[1], T Tsuruga[1], K Nagasaka[1], Y Matsumoto[1], Y Ikeda[1], K Shoji[1], K Oda[1], H Fukuhara[2], K Nakagawa[3], S Kato[4], T Yano[1] and Y Taketani[1]

[1]Department of Obstetrics and Gynecology, Graduate School of Medicine, The University of Tokyo, 7-3-1 Hongo, Bunkyo-ku, Tokyo 113-8655, Japan; [2]Department of Urology, Graduate School of Medicine, The University of Tokyo, 7-3-1 Hongo, Bunkyo-ku, Tokyo 113-8655, Japan; [3]Department of Radiology, Graduate School of Medicine, The University of Tokyo, 7-3-1 Hongo, Bunkyo-ku, Tokyo 113-8655, Japan; [4]Institute of Molecular and Cellular Biosciences, The University of Tokyo, 1-1-1 Yayoi, Bunkyo-ku, Tokyo 113-0034, Japan

BACKGROUND: The TFII-I is a multifunctional transcriptional factor known to bind specifically to several DNA sequence elements and to mediate growth factor signalling. A microdeletion at the chromosomal location 7q11.23 encoding TFII-I and the related family of transcription factors may result in the onset of Williams–Beuren syndrome, an autosomal dominant genetic disorder characterised by a unique cognitive profile, diabetes, hypertension, anxiety, and craniofacial defects. Hereditary breast and ovarian cancer susceptibility gene product BRCA1 has been shown to serve as a positive regulator of SIRT1 expression by binding to the promoter region of SIRT1, but cross talk between BRCA1 and TFII-I has not been investigated to date.

METHODS: A physical interaction between TFII-I and BRCA1 was explored. To determine pathophysiological function of TFII-I, its role as a transcriptional cofactor for BRCA1 was investigated.

RESULTS: We found a physical interaction between the carboxyl terminus of TFII-I and the carboxyl terminus of BRCA1, also known as the BRCT domain. Endogenous TFII-I and BRCA1 form a complex in nuclei of intact cells and formation of irradiation-induced nuclear foci was observed. We also showed that the expression of TFII-I stimulates the transcriptional activation function of BRCT by a transient expression assay. The expression of TFII-I also enhanced the transcriptional activation of the SIRT1 promoter mediated by full-length BRCA1.

CONCLUSION: These results revealed the intrinsic mechanism that TFII-I may modulate the cellular functions of BRCA1, and provide important implications to understand the development of breast cancer.

British Journal of Cancer (2011) **104,** 1349–1355. doi:10.1038/bjc.2011.75 www.bjcancer.com
Published online 15 March 2011

Keywords: TFII-I; BRCA1; interaction; activation; DNA damage repair

The TFII-I was identified originally as a factor that could bind to two distinct promoter elements, the pyrimidine-rich initiator and the recognition site (E-box) for upstream factor 1. The TFII-I stimulates transcription from the potent TATA- and initiator-containing adenovirus major late promoter (AdMLP) synergistically with upstream factor 1 (Roy *et al*, 1997). The TFII-I is a unique multifunctional factor that selectively regulates gene expressions when activated by a variety of extracellular signals and can function both as a basal transcriptional factor and as an activator (Roy, 2007). An autosomal dominant genetic disorder Williams–Beuren syndrome is a multisystem disorder characterised by distinctive facial features, mental disability, diabetes mellitus, and supravalvular aortic stenosis. The haploinsufficiency for TFII-I is causative to the craniofacial phenotype in humans (Pober, 2010). The primary structure of TFII-I is compatible with its multifunctional properties, consisting of six direct reiterated I-repeats, R1–R6, each containing a putative helix-loop-helix motif (Roy, 2007). The I-repeats are postulated to be protein interaction surfaces. Given those multifunctional features and structural characteristics, it is important to investigate the role of the I-repeats in mediating protein interactions and to search for proteins that make complex with TFII-I through this domain.

The breast cancer susceptibility gene *BRCA1* encodes a phosphoprotein that is involved in ubiquitination, DNA damage response, regulation of cell cycle checkpoints, and transcriptional regulation. Binding to the transcriptional machinery by the carboxyl terminal BRCA1, referred to as BRCT domain, was the first biochemical activity ascribed to the BRCA1 protein (Anderson *et al*, 1998). In addition, BRCT has been shown to be involved in double-stranded DNA repair and homologous recombination (Callebaut and Mornon, 1997; Moynahan *et al*, 1999; Zhong *et al*, 1999). On the basis of the data that targeted deletion of the BRCT domain results in embryonic lethality (Hohenstein *et al*, 2001), BRCT is postulated to be indispensable for the normal cellular growth, and it would be intriguing to investigate physiological functions of BRCT. BRCA1 carboxyl-terminal domain (BRCT) possesses the autonomous transcriptional activation

*Correspondence: Dr O Wada-Hiraike; E-mail: osamu.hiraike@gmail.com
Received 22 October 2010; revised 31 January 2011; accepted 8 February 2011; published online 15 March 2011

function when the BRCT domain is fused to a GAL4 DNA-binding domain (Monteiro *et al*, 1996). The point mutations in the BRCT domain derived from patients with inherited breast cancer result in loss of transcriptional activity (Chapman and Verma, 1996). The BRCT domain has been shown to be an interaction surface with a number of transcription factors and co-regulators (Saka *et al*, 1997; Wada *et al*, 2004; Oishi *et al*, 2006; Hiraike *et al*, 2010).

To better understand the functional significance and the transcriptional regulation of BRCT, we previously have searched for putative transcription coactivator complexes that interact with the BRCT domain using a biochemical approach (Wada *et al*, 2004; Oishi *et al*, 2006). During these studies, we preliminary found that TFII-I interacted with the BRCT domain. Here, we confirmed that the carboxyl terminus of TFII-I and BRCA1 form a complex *in vivo*. We further studied the effect on transcriptional regulation of BRCA1 driven by TFII-I. These findings establish a principal biological function of TFII-I as an activator of BRCA1 function, and identify TFII-I as a possible determinant of breast cancer.

MATERIALS AND METHODS

Cell culture

Human cervical adenocarcinoma HeLa (CCL-2), HCC1937 (CRL-2336) breast cancer cells that express a carboxyl-terminally truncated BRCA1 protein (Scully *et al*, 1999), and African green monkey kidney fibroblast-like COS7 (CRL-1651) cell lines were purchased from the American Type Culture Collection (Manassas, VA, USA). HeLa and COS7 cells were maintained in Dulbecco's modified Eagle medium supplemented with 10% fetal bovine serum. HCC1937 cells were maintained in RPMI medium supplemented with 10% fetal bovine serum.

Plasmid construction

BRCA1 expression vectors, BRCT vectors and reporter constructs (17M8-AdMLP-luc and SIRT1-luc) were described previously (Wada *et al*, 2004; Hiraike *et al*, 2010). TFII-I expression vectors were described previously (Cheriyath and Roy, 2001).

Chemicals and antibodies

Rabbit antibodies were anti-TFII-I, anti-BRCA1, and anti-GST (Cell Signaling Technology Inc., Temecula, CA, USA, catalogue no. #4562, #9010, and #2622, respectively). Mouse monoclonal antibodies were anti-BRCA1 (Calbiochem, EMD Biosciences Inc., La Jolla, CA, USA, catalogue no. OP107), anti-SIRT1 (Abcam Ltd., Cambridge, UK, catalogue no. ab32441), and HRP-conjugated anti-Flag (Abcam Ltd., catalogue no. ab49763). Anti-BRCA1 (catalogue no. sc-642), anti-p53 (catalogue no. sc-126), and anti-Actin (catalogue no. sc-47778) were purchased from Santa Cruz Biotechnology Inc. (Santa Cruz, CA, USA). Alexa Fluor 488 conjugated donkey anti-mouse IgG (catalogue no. A-21202) and Alexa Fluor 568 conjugated goat anti-rabbit IgG (catalogue no. A-11011) were purchased from Invitrogen (Carlsbad, CA, USA).

Immunoprecipitation and western blot

The formation of a TFII-I-BRCA1 complex in HeLa, HCC1937, and COS7 cells was analysed by immunoprecipitation. The whole-cell extracts of HeLa and HCC1937 cells were applied for immunoprecipitation with anti-BRCA1 antibodies or preimmune IgG. The immunoprecipitates were subjected to 30 μl of protein G sepharose 4 Fast Flow (GE healthcare UK Ltd., Buckinghamshire, UK) and subsequently immunoblotted by anti-TFII-I antibodies. Reciprocal immunoprecipitation was also performed. COS7 cells transfected with indicated plasmids were lysed, fractionated, and subjected to anti-FLAG M2 agarose (Sigma-Aldrich, St Louis, MO, USA). Immunoprecipitated materials were blotted with anti-GST antibodies to identify TFII-I-containing complexes.

RNAi

The ablation of TFII-I and BRCA1 was performed by transfection of HeLa cells with siRNA duplex oligos synthesised by Qiagen (Hilden, Germany). Cells were transfected with control siRNA (AllStars Negative Control siRNA, 1027281), TFII-I-specific siRNA (TFII-I-RNAi: 5′-AAACGGAGCCUACUGAACA-3′, which covered mRNA regions of nucleotides 956–974 (amino acids 195–201) of TFII-I), DBC1-specific siRNA (DBC1-RNAi: 5′-AAACGGAGCCUA CUGAACA-3′, which covered mRNA regions of nucleotides 1379–1397 (amino acids 460–466) of DBC1), and BRCA1-specific siRNA (SI02664361) using HiperFect reagent (Qiagen).

GST-pull down assay

Glutathione-S-transferase fusion proteins or GST alone were expressed in *Escherichia coli* and immobilised on glutathione-sepharose 4B beads (GE healthcare UK Ltd.). The GST proteins were incubated with nuclear extracts of HeLa cells. Unbound proteins were removed and specifically bound proteins were eluted and analysed by SDS–PAGE.

Luciferase assay

Transfection was performed with Effectene reagent (Qiagen) or Lipofectamine 2000 (Invitrogen) according to the manufacturer's recommendation. For luciferase assay, cells were transfected with indicated expression vectors and/or GAL4 vectors. Reporter plasmids (17M8-AdMLP-luc or SIRT1-luc) were also cotransfected. As an internal control to equalise transfection efficiency, phRL CMV-*Renilla* vector (Promega Co., Madison, WI, USA) was also transfected in all the experiments. Individual transfections, each consisting of triplicate wells, were repeated at least three times as described previously (Wada *et al*, 2004).

Fluorescence microscopy

HeLa cells were grown on 12 mm BD BioCoat glass coverslips (BD Biosciences, San Jose, CA, USA, 354085) in 6-well plates. The cells were exposed to 8-gray (Gy) of γ-irradiation, fixed with PBS containing 4% paraformaldehyde and permeabilised in PBS with 0.2% (v/v) Triton X-100. After blocking, the cells were incubated sequentially with anti-BRCA1 and anti-TFII-I antibodies. Secondary antibodies were Alexa Fluor 488 conjugated donkey anti-mouse IgG, or Alexa Fluor 568 conjugated goat anti-rabbit IgG. The slides were briefly counter-stained and analysed under the confocal fluorescence microscope (Carl-Zeiss MicroImaging Inc., Oberkochen, Germany). Quantification of colocalisation was analysed using LSM7 series-ZEN200x software (Carl-Zeiss Micro-Imaging Inc.), and the ratio of colocalisation pixels *vs* total pixels in the target area was measured.

Chromatin immunoprecipitation assay

Preparation of soluble HeLa chromatin for PCR amplification was performed essentially as described (Oishi *et al*, 2006; Hiraike *et al*, 2010). Subconfluent HeLa cells were cross-linked with 1.5% formaldehyde at room temperature for 15 min, and washed twice with ice-cold PBS. The cell pellet was then resuspended in 0.2 ml lysis buffer and sonicated by Bioruptor UCD-250 (Cosmo Bio Co. Ltd., Tokyo, Japan). The sheared soluble chromatin was then subjected to immunoprecipitation with specific antibodies and protein G-sepharose equilibrated with salmon sperm DNA (Millipore, Upstate, Billerica, MA, USA). After extensive wash,

the beads were eluted. The eluate was incubated for 6 h at 65°C to reverse the formaldehyde cross-linking. The extracted DNA was purified with the use of QIAquick PCR purification kit (Qiagen). Polymerase chain reaction was performed using specific primers for the SIRT1 promoter (Wang *et al*, 2008; Hiraike *et al*, 2010) and the p21 promoter (Oishi *et al*, 2006).

RESULTS

TFII-I and BRCA1 interact *in vivo*

The pull-down products of nuclear extracts from HeLa cells through GST-BRCT column were separated by SDS–PAGE. In consistent with our preliminary result, we confirmed that TFII-I proteins interact with GST-BRCT by western blot (Figure 1A). To determine the interaction between the endogenous TFII-I and BRCA1 in cultured human cells, whole-cell lysates of HeLa cells were immunoprecipitated with anti-BRCA1 antibodies (epitope mapping at the carboxyl-terminus of BRCA1). The immunoblotting analysis using anti-TFII-I antibodies revealed the existence of TFII-I in cell lysate immunoprecipitates (Figure 1B, 1), which indicates that TFII-I physically associates with BRCA1 in living cells. The whole-cell extracts of HCC1937 cells known to lack last BRCT domain were also immunoprecipitated with anti-BRCA1 antibodies (epitope mapping at the amino-terminus of BRCA1). The immunoblotting analysis revealed the absence of TFII-I in cell lysate immunoprecipitates, which reinforced the importance of BRCT domain as the interaction surface with TFII-I (Figure 1B, 2). These data indicated that TFII-I interacted with BRCA1 through the BRCT domain. Reciprocal immunoprecipitation analysis confirmed this association (Figure 1B, 3).

To identify the regions of TFII-I that are responsible for the interaction with BRCT, deletion mutants of TFII-I were used for the assay. COS7 cells were transfected with Flag-tagged BRCA1 and GST-tagged TFII-I and nuclear extracts of transfected cells were immunoprecipitated with the anti-FLAG M2 agarose beads. Western blotting analysis with anti-GST antibodies revealed the existence of GST-tagged TFII-I in the protein extract of immunoprecipitates (Figure 1C), confirming that BRCA1 forms a complex with TFII-I. Flag-tagged BRCA1 and deletion mutants of GST-tagged TFII-I were also subjected to immunoprecipitation. TFII-I lacking the amino terminal region (TFII-I ΔN90) also interacted with BRCA1, while TFII-I lacking carboxyl terminus (TFII-I p70 and p46) showed no interaction with BRCA1. Immunoprecipitation using cytoplasmic fraction of the COS7 cells was also performed and TFII-I was not co-immunoprecipitated with BRCA1. These findings indicate that the carboxyl terminus (R3-R6) of TFII-I and the BRCT domain are both necessary and sufficient for the interaction between TFII-I and BRCA1 in cultured cells.

TFII-I and BRCA1 form endogenous complex in intact cells and nuclear foci in DNA-damaged cells

As BRCA1 and TFII-I interact *in vivo*, it was of interest to examine the subcellular distribution of these two proteins. To this end, immunofluorescence analysis was performed on HeLa cells. More than 80% substantial colocalisation signal (Merge) of BRCA1 (Alexa Fluor 488-conjugated anti-mouse IgG, green) and TFII-I (Alexa Fluor 568-conjugated anti-rabbit IgG, red) was observed in nuclei in control cells. Therefore, protein complexes containing both BRCA1 and TFII-I are likely to be distributed throughout nuclei. This result also implied the importance of nuclear localisation signal for the colocalisation of BRCA1 and TFII-I in nuclei. The previous study demonstrated that BRCA1 has been shown to display discrete nuclear foci after treatment of cells with irradiation (Zhong *et al*, 1999). HeLa cells irradiated with 8-Gy γ radiation demonstrated the punctate pattern of immunostaining

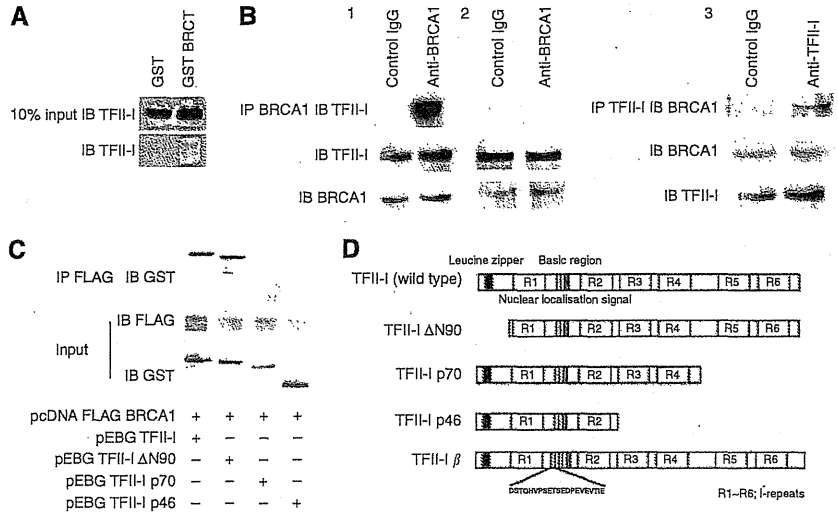

Figure 1 *In vivo* and *in vitro* association between TFII-I and BRCA1, and mapping of the BRCT-interacting region of TFII-I. (**A**) Identification of the interaction between BRCT and TFII-I using GST-BRCT. Bacterially expressed GST fusion proteins immobilised on beads were used in *in vitro* pull-down assays. Nuclear extracts of HeLa cells were incubated with GST-BRCT. The beads were extensively washed, and followed by immunoblotting (IB) using anti-TFII-I antibodies. (**B**) The complex formation of TFII-I and BRCA1 in HeLa cells was analysed by co-immunoprecipitation (IP) with the antibodies to BRCA1 (epitope mapping at the carboxyl-terminus of BRCA1). The immunoblotting analysis using anti-TFII-I antibodies revealed the existence of TFII-I in cell lysate immunoprecipitates (Figure 1B, 1), which indicates that TFII-I physically associates with BRCA1 in living cells. Reciprocal immunoprecipitation analysis confirmed the association of TFII-I and BRCA1 (Figure 1B, 3). The whole-cell extracts of HCC1937 cells known to lack last BRCT domain were also immunoprecipitated with anti-BRCA1 antibodies (epitope mapping at the amino-terminus of BRCA1). The immunoblotting analysis revealed the absence of TFII-I in cell lysate immunoprecipitates (Figure 1B, 2), indicating the importance of BRCT as a binding surface of TFII-I. (**C**) Mapping of the BRCT-interaction region of TFII-I. COS7 cells were transfected with GST-tagged TFII-I (wild type, ΔN90, p70, and p46) and Flag-tagged BRCA1 expression vectors. Nuclear extracts of transfected COS7 cells were prepared and the complex formation of TFII-I and BRCA1 was analysed by IP with the anti-Flag M2 agarose beads, followed by IB using anti-GST antibodies. (**D**) A schematic diagram of the structure of TFII-I (wild type, ΔN90, p70, p46, and β isoform) is shown.

for BRCA1 and this pattern overlap TFII-I-containing foci in HeLa cells (Figure 2B, 1–3). These data indicated that double strand DNA damage lead to the nuclear accumulation of the BRCA1-TFII-I complex, possibly at the site of double strand DNA-damage.

TFII-I enhances the transcriptional activation of BRCT

The result that the BRCT domain interacts with TFII-I led us to examine role of TFII-I in the transactivation function of GAL4-fused BRCT. Transient transfection assays were performed using a 17M8-AdMLP-luc luciferase reporter plasmid, carrying eight tandem repeat GAL4 DNA-binding sites (17M × 8) upstream of AdMLP driving expression of the firefly luciferase gene. The TFII-I alone had no effect on this luciferase reporter construct (Figure 3, lanes 2–6). Although GAL4-BRCT fusion protein (GAL-BRCT) activated the promoter activity of the reporter plasmid in COS7 cells, the transcriptional activity of BRCT was significantly stimulated by the expression of TFII-I at best two-fold on the artificial promoter in luciferase assays (Figure 3, lanes 7–8). Although TFII-I ΔN90 possessing the BRCT binding domain stimulated the transcriptional activation of GAL-BRCT, TFII-I lacking an interaction domain with BRCA1 (TFII-I p70 and p46) lost its ability to stimulate the BRCT-mediated transcriptional activation (Figure 3, lanes 9–11). The mammalian TFII-I has four spliced isoforms: α, β, γ, and Δ (wild type). Upon serum starvation, the β and Δ isoforms exhibits subcellular distribution changes in murine NIH3T3 cells (Hakre *et al*, 2006). The experimental data showed that TFII-I β also stimulated the transcriptional activation of BRCT (Figure 3, lane 12). These results suggest that carboxyl terminus of TFII-I has a significant role in the stimulation of BRCT-dependent transactivation.

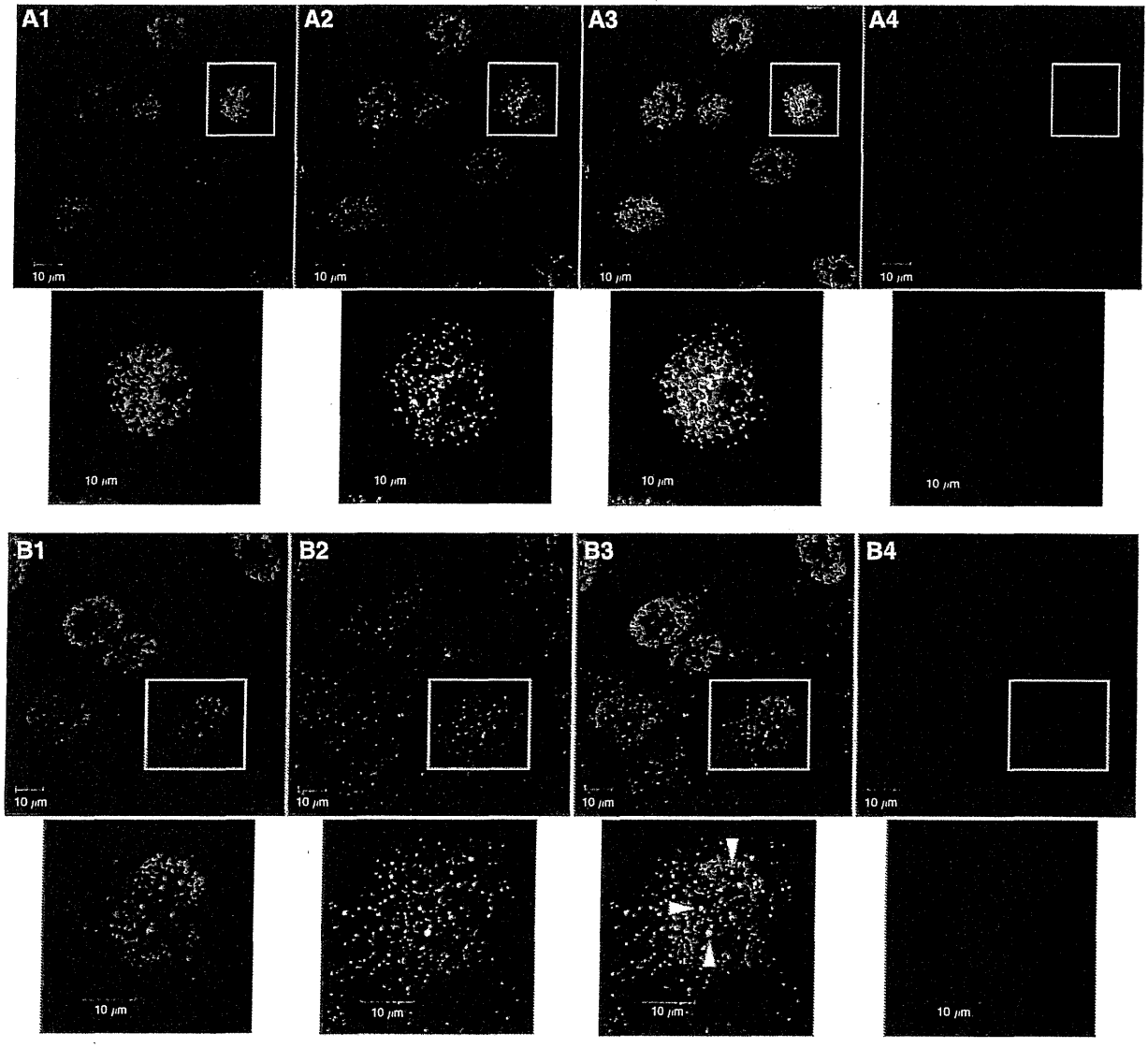

Figure 2 Colocalisation of BRCA1 and TFII-I in HeLa cells. (**A**–**D**) HeLa cells were either treated by 8-Gy of gamma-irradiation or none, fixed, and permeabilised. The cells were incubated with primary antibodies and subsequently with secondary antibodies. The expression of BRCA1 (green) and TFII-I (red) was investigated under the confocal fluorescence microscopy (Carl-Zeiss). Representative immunofluorescence studies are shown (**A**, control cells; **B**, irradiated cells; 1, TFII-I; 2, BRCA1; 3, merge; 4, 4′, 6-diamino-2-phenylindole staining). Arrows in B3 indicate a cell showing nuclear foci formation of TFII-I and BRCA1. Bars indicate 10 μm.

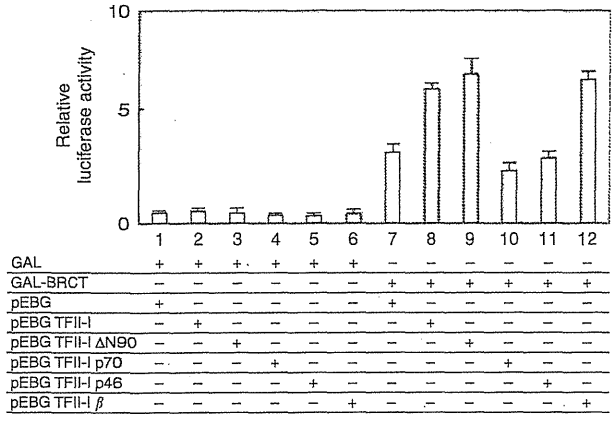

Figure 3 TFII-I stimulates transcription of GAL4-BRCT through its carboxyl-terminal domain. Transient transfection assays were performed to examine the cofactor activity of TFII-I in the transactivation function of GAL4-fused BRCT. COS7 cells were transfected with the indicated combinations of mammalian expression plasmids. At 24 h after transfection, the cells were harvested, and transfected whole-cell lysates were assayed for luciferase activity produced from the reporter plasmid (17M8-AdMLP-luc). TFII-I showed a specific stimulation of the transactivation function of BRCT. Carboxyl-terminus of TFII-I was indispensable for this stimulation of BRCT. The phRL *Renilla* CMV-luc vector was transfected as a control of transfection efficiency. Each experiment was repeated at least three times in triplicate. Error bars represent s.d.

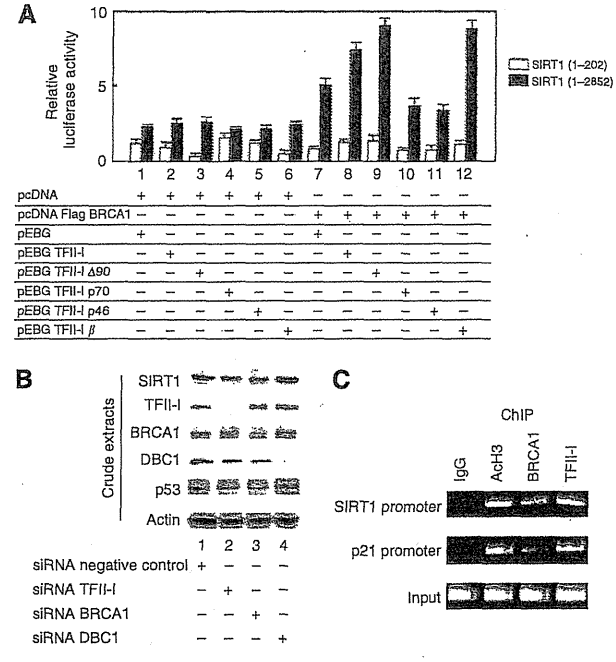

Figure 4 TFII-I stimulates transcription by BRCA1 through its carboxyl-terminal domain. (**A**) Transient transfection assays were performed to examine the influence of TFII-I using an artificial luciferase reporter constructs. COS7 cells were transfected with the indicated combinations of mammalian expression plasmids. At 24 h after transfection, cells were harvested, and transfected whole-cell lysates were assayed for luciferase activity produced from the reporter plasmids. Full-length TFII-I and TFII-I ΔN90 showed specific upregulation of SIRT1 (1-2852)-luciferase activity mediated by BRCA1, while TFII-I p70 and TFII-I p46, lacking BRCT-interaction region, had no effect on SIRT1-luciferase activity. TFII-I showed no effect on SIRT1 (1-202)-luciferase activity that lack the binding domain of BRCA1. (**B**) The siRNA-mediated knockdown of BRCA1 decreased the expression of SIRT1. Knockdown of TFII-I also resulted in downregulation of SIRT1. Expression of BRCA1 and p53 was decreased by depletion of TFII-I. HeLa cells were transfected with indicated siRNA. At 48 h after transfection, cells were harvested and analysed by western blotting. (**C**) Chromatin immunoprecipitation assay was performed to confirm the recruitment of BRCA1 and TFII-I at the SIRT1 gene promoter and the p21 gene promoter. Both promoter regions are known to recruit BRCA1.

TFII-I enhances BRCA1-mediated SIRT1 expression

The previous chromatin immunoprecipitation assay showed that BRCA1 interacted with the SIRT1 promoter region between 1354 and 1902 and this binding resulted in elevated expression of SIRT1 (Wang *et al*, 2008; Hiraike *et al*, 2010). We explored whether TFII-I has an effect on the BRCA1-mediated stimulation of the SIRT1 promoter and demonstrated that the BRCA1-mediated stimulation of the SIRT1 promoter was specifically upregulated by exogenous expression of TFII-I although the impact of TFII-I was rather less on SIRT1 promoter compared with AdMLP (Figure 4A, lane 8). The TFII-I p70 and p46 showed no influence to enhance the BRCA1-mediated transactivation of SIRT1-luciferase reporter constructs, but TFII-I ΔN90 showed enhancement on the SIRT1-luciferase transactivation function mediated by BRCA1 (Figure 4, lanes 9–11). The TFII-I β was also able to stimulate the SIRT1-luciferase transcriptional activation function mediated by BRCA1 (Figure 4, lane 12). Interaction of BRCA1 with the SIRT1 promoter region was postulated to be important for the activation function of TFII-I because SIRT1-luciferase (1–202) reporter constructs lacking the BRCA1-interaction site showed no enhancement of luciferase activity.

We next examined the effect of siRNA-mediated depletion of TFII-I or BRCA1 on their downstream genes. Knockdown of BRCA1 expression by BRCA1-specific siRNA abrogated the expression of SIRT1 (Figure 4B, lane 3), validating the previous report that the expression of SIRT1 is indeed dependent on BRCA1 (Wang *et al*, 2008). As shown in Figure 4B, lane 2, depletion of the endogenous TFII-I also decreased the expression of SIRT1. Thus, our data demonstrate that TFII-I has a critical role in regulating downstream gene expressions dependent on BRCA1 *in vivo*. Depletion of TFII-I resulted in downregulation of p53 and BRCA1, suggesting a role of TFII-I in DNA damage response (Figure 4B, lane 2).

To test whether TFII-I and BRCA1 were indeed recruited to the SIRT1 promoter, we performed a chromatin immunoprecipitation assay using the SIRT1 gene promoter 1354–1902, a region known to recruit BRCA1 (Wang *et al*, 2008; Hiraike *et al*, 2010) and the p21 gene promoter (Oishi *et al*, 2006). As expected, clear recruitment of endogenous TFII-I and BRCA1 to the target sequence (1354–1902) in the SIRT1 and the p21 promoter was observed in HeLa cells (Figure 4C).

DISCUSSION

The TFII-I is considered to have important roles in regulating the expression of genes as a signal-induced multifunctional transcription factor (Hakre *et al*, 2006; Roy, 2007). Here, we demonstrated that endogenous TFII-I associated with BRCA1, which suggests the possibility that TFII-I has a functional relationship with BRCA1-related phenotypical changes. This interaction between BRCA1 and TFII-I was physiologically functional because our results demonstrated that the TFII-I-containing complex stimulated the autonomous transcriptional activity of BRCT.

The transcriptional activation function of BRCT is considered to be a key to its tumour suppressor activity (Chapman and Verma, 1996; Monteiro *et al*, 1996) because a point mutation within the BRCT domain (A1708E), lacking transactivation function, was shown to be critical for a DNA damage response by the treatment with methylmethane sulfonate (Zhong *et al*, 1999). The importance

of BRCT for transcriptional control and growth suppression is also highlighted by the fact that cancer associated mutations attenuated both, but neutral polymorphism did not (Humphrey *et al*, 1997). The BRCT domain is found in a diverse group of proteins implicated in DNA repair and cell cycle check-point control (Bork *et al*, 1997; Callebaut and Mornon, 1997). BRCA1 carboxyl-terminal domain possesses an autonomous folding unit defined by conserved clusters of hydrophobic amino acids, and BRCT is likely to represent a protein interaction surface (Saka *et al*, 1997). Thus, activation of BRCT has implications both in anti-tumorigenic and in DNA repair processes. Anti-tumorigenic role of TFII-I is also supported by the finding that TFII-I inhibits the growth of MCF-7 (Ogura *et al*, 2006). The study had shown that TFII-I down-regulates a subset of oestrogen-responsive genes, only those containing initiator elements, by recruiting oestrogen receptor α and co-repressors to these promoters. Therefore, TFII-I is not thought to be a general activator of transcription and the transcriptional control by TFII-I would be promoter-dependent manner. The transcriptional regulation played by TFII-I may be complicated because TFII-I was shown to co-immunoprecipitates with transcriptional repressor, histone deacetylase 3 (Wen *et al*, 2003).

We also have shown that TFII-I and BRCA1 colocalise in nuclei of irradiated cells. Previous studies indicated that BRCA1 responds to the repair of DNA by homologous recombination. The BRCA1 associates with RAD51 in subnuclear clusters (Zhong *et al*, 1999). The RAD51 is postulated to be a key component of the mechanism in which DNA damage is repaired by homologous recombination. When cells are exposed to ionising radiation, both BRCA1 and RAD51 localise to the damaged region, and both BRCA1 and RAD51 initiate homologous recombination and the repair of double-strand breaks. Our data that TFII-I and BRCA1 formed nuclear foci after irradiation treatment may suggest that both BRCA1 and TFII-I participates in the DNA damage repair pathway. These data are consistent with the previous observation that TFII-I influences persistence of γ-H2AX foci and thus affects double strand break repair, suggesting a role for TFII-I in DNA repair (Desgranges and Roy, 2006). Our results also indicated that TFII-I promoted BRCA1-dependent transcriptional regulation because SIRT1-luciferase activity was potentiated by the ectopic expression of TFII-I. The TFII-I would serve as a transcriptional activation factor to manipulate transcriptions, thereby influencing transcriptional products such as SIRT1. These results also suggest the possible mechanism how TFII-I regulates DNA damage machinery because SIRT1 possesses DNA repair activity (Jeong *et al*, 2007). In consistent with these data, depletion of endogenous TFII-I resulted in a decreased expression of p53 and BRCA1. We have to further confirm the effect of DNA damage response when TFII-I is abrogated to show its involvement in this mechanism. Our results showed a new insight that TFII-I may serve, at least in part, as DNA damage response machinery.

In conclusion, our data indicate that TFII-I have an important role in regulating BRCA1-mediated functions through binding to the BRCT domain and it may be probable that TFII-I is involved in anti-tumorigenic processes. The meaning of TFII-I functions would be apparent by evaluating its expression in tumour tissues such as breast cancer. The expression of TFII-I would be therapeutically beneficial by affecting different TFII-I-mediated regulatory pathways together with BRCA1 and the failure of binding between BRCA1 and TFII-I may be a key event in cancer predisposition.

ACKNOWLEDGEMENTS

This study was supported by a Grant-in-Aid for Scientific Research from the Ministry of Education, Science and Culture, JMS Bayer Schering Pharma Grant, and Kowa Life Science Foundation, Japan. We thank Dr RG Roeder (The Rockefeller University) for TFII-I expression vectors and Dr AL Roy (Tufts University School of Medicine) for TFII-I expression vectors and deletion mutants.

REFERENCES

Anderson SF, Schlegel BP, Nakajima T, Wolpin ES, Parvin JD (1998) BRCA1 protein is linked to the RNA polymerase II holoenzyme complex via RNA helicase A. *Nat Genet* **3:** 254–256

Bork P, Hofmann K, Bucher P, Neuwald AF, Altschul SF, Koonin EV (1997) A superfamily of conserved domains in DNA damage-responsive cell cycle checkpoint proteins. *FASEB J* **11:** 68–76

Callebaut I, Mornon JP (1997) From BRCA1 to RAP1: a widespread BRCT module closely associated with DNA repair. *FEBS Lett* **400:** 25–30

Chapman MS, Verma IM (1996) Transcriptional activation by BRCA1. *Nature* **382:** 678–679

Cheriyath V, Roy AL (2001) Structure-function analysis of TFII-I. Roles of the N-terminal end, basic region, and I-repeats. *J Biol Chem* **276:** 8377–8383

Desgranges ZP, Roy AL (2006) TFII-I: connecting mitogenic signals to cell cycle regulation. *Cell Cycle* **5:** 356–359

Hakre S, Tussie-Luna MI, Ashworth T, Novina CD, Settleman J, Sharp PA, Roy AL (2006) Opposing functions of TFII-I spliced isoforms in growth factor-induced gene expression. *Mol Cell* **24:** 301–308

Hiraike H, Wada-Hiraike O, Nakagawa S, Koyama S, Miyamoto Y, Sone K, Tanikawa M, Tsuruga T, Nagasaka K, Matsumoto Y, Oda K, Shoji K, Fukuhara H, Saji S, Nakagawa K, Kato S, Yano T, Taketani Y (2010) Identification of DBC1 as a transcriptional repressor for BRCA1. *Br J Cancer* **102:** 1061–1067

Hohenstein P, Kielman MF, Breukel C, Bennett LM, Wiseman R, Krimpenfort P, Cornelisse C, van Ommen GJ, Devilee P, Fodde R (2001) A targeted mouse Brca1 mutation removing the last BRCT repeat results in apoptosis and embryonic lethality at the headfold stage. *Oncogene* **20:** 2544–2550

Humphrey JS, Salim A, Erdos MR, Collins FS, Brody LC, Klausner RD (1997) Human BRCA1 inhibits growth in yeast: potential use in diagnostic testing. *Proc Natl Acad Sci USA* **94:** 5820–5825

Jeong J, Juhn K, Lee H, Kim SH, Min BH, Lee KM, Cho MH, Park GH, Lee KH (2007) SIRT1 promotes DNA repair activity and deacetylation of Ku70. *Exp Mol Med* **39:** 8–13

Monteiro AN, August A, Hanafusa H (1996) Evidence for a transcriptional activation function of BRCA1 C-terminal region. *Proc Natl Acad Sci USA* **93:** 13595–13599

Moynahan ME, Chiu JW, Koller BH, Jasin M (1999) Brca1 controls homology-directed DNA repair. *Mol Cell* **4:** 511–518

Ogura Y, Azuma M, Tsuboi Y, Kabe Y, Yamaguchi Y, Wada T, Watanabe H, Handa H (2006) TFII-I down-regulates a subset of estrogen-responsive genes through its interaction with an initiator element and estrogen receptor alpha. *Genes Cells* **11:** 373–381

Oishi H, Kitagawa H, Wada O, Takezawa S, Tora L, Kouzu-Fujita M, Takada I, Yano T, Yanagisawa J, Kato S (2006) An hGCN5/TRRAP histone acetyltransferase complex co-activates BRCA1 transactivation function through histone modification. *J Biol Chem* **281:** 20–26

Pober BR (2010) Williams-Beuren syndrome. *N Engl J Med* **362:** 239–252

Roy AL (2007) Signal-induced functions of the transcription factor TFII-I. *Biochim Biophys Acta* **1769:** 613–621

Roy AL, Du H, Gregor PD, Novina CD, Martinez E, Roeder RG (1997) Cloning of an inr- and E-box-binding protein, TFII-I, that interacts physically and functionally with USF1. *EMBO J* **16:** 7091–7104

Saka Y, Esashi F, Matsusaka T, Mochida S, Yanagida M (1997) Damage and replication checkpoint control in fission yeast is ensured by interactions of Crb2, a protein with BRCT motif, with Cut5 and Chk1. *Genes Dev* **11:** 3387–3400

Scully R, Ganesan S, Vlasakova K, Chen J, Socolovsky M, Livingston DM (1999) Genetic analysis of BRCA1 function in a defined tumor cell line. *Mol Cell* **4:** 1093–1099

Wada O, Oishi H, Takada I, Yanagisawa J, Yano T, Kato S (2004) BRCA1 function mediates a TRAP/DRIP complex through direct interaction with TRAP220. *Oncogene* **23:** 6000–6005

Wang RH, Zheng Y, Kim HS, Xu X, Cao L, Luhasen T, Lee MH, Xiao C, Vassilopoulos A, Chen W, Gardner K, Man YG, Hung MC, Finkel T, Deng CX (2008) Interplay among BRCA1, SIRT1, and Survivin during BRCA1-associated tumorigenesis. *Mol Cell* **32:** 11–20

Wen YD, Cress WD, Roy AL, Seto E (2003) Histone deacetylase 3 binds to and regulates the multifunctional transcription factor TFII-I. *J Biol Chem* **278:** 1841–1847

Zhong Q, Chen CF, Li S, Chen Y, Wang CC, Xiao J, Chen PL, Sharp ZD, Lee WH (1999) Association of BRCA1 with the hRad50-hMre11-p95 complex and the DNA damage response. *Science* **285:** 747–750

β-catenin (*CTNNB1*) S33C Mutation in Ovarian Microcystic Stromal Tumors

Daichi Maeda, MD, PhD, Junji Shibahara, MD, PhD,* Takahiko Sakuma, MD, PhD,† Masanori Isobe, MD,‡ Shinichi Teshima, MD,§ Masaya Mori, MD,‖ Katsutoshi Oda, MD, PhD,¶ Shunsuke Nakagawa, MD, PhD,¶ Yuji Taketani, MD, PhD,¶ Shumpei Ishikawa, MD, PhD,* and Masashi Fukayama, MD, PhD**

Abstract: Microcystic stromal tumor (MCST) is a recently described subtype of ovarian tumor characterized by prominent microcystic histologic pattern and diffuse immunoreactivity for CD10 and vimentin. However, its pathobiology, particularly its histogenesis, remains largely unclear. Here, we report 2 cases of ovarian MCST, in which we have performed extensive histologic, immunohistochemical, and genetic investigations to determine its distinct nature among ovarian neoplasms. The patients were 32 and 41 years of age. Both tumors were solid and cystic masses involving the right ovary. Microscopically, tumor cells with generally bland, round-to-ovoid nuclei grew in microcystic, macrocystic, and solid patterns. Intervening thick fibrous stroma was observed. Immunohistochemically, tumor cells were diffusely and strongly positive for CD10, vimentin, and Wilms tumor 1. Furthermore, we detected aberrant nuclear expression of β-catenin protein in both cases. Of interest, mutation analyses revealed the presence of an identical point mutation, c.98C > G, in exon 3 of β-catenin (*CTNNB1*) in both tumors. This is an oncogenic mutation that causes replacement of serine with cysteine at codon 33, leading to the loss of a phosphorylation site in the β-catenin protein. The results of this study strongly suggest that dysregulation of the Wnt/β-catenin pathway plays a fundamental role in the pathogenesis of ovarian MCST. Finally, by comparing the immunophenotype of MCST with its histologic mimics and other ovarian sex cord-stromal tumors, we were able to identify unique features of MCST and a panel of markers useful in differential diagnosis.

From the *Department of Pathology, Graduate School of Medicine; ¶Department of Obstetrics and Gynecology, Faculty of Medicine, The University of Tokyo; §Department of Pathology, Doai Memorial Hospital; ‖Department of Pathology, Mitsui Memorial Hospital, Tokyo; †Department of Diagnostic Pathology; and ‡Department of Obstetrics and Gynecology, Osaka Rosai Hospital, Sakai, Japan.

Conflicts of Interest and Source of Funding: The authors have disclosed that they have no significant relationships with, or financial interest in, any commercial companies pertaining to this article. This study was supported by a Grant-in-Aid for Scientific Research (KAKENHI) from the Japan Society for the Promotion of Science.

Correspondence: Masashi Fukayama, MD, PhD, Department of Pathology, Graduate School of Medicine, The University of Tokyo, 7-3-1 Hongo Bunkyoku, Tokyo 113-0033, Japan (e-mail: mfukayama-tky@umin.net).

Key Words: microcystic stromal tumor, ovary, β-catenin

(*Am J Surg Pathol* 2011;35:1429–1440)

In 2009, Irving and Young[7] reported a series of ovarian neoplasms that they described as "superficially reminiscent of thecoma in some regions, but with a microcystic pattern often so conspicuous that it dwarfed the thecoma-like regions." On the basis of the distinctive histologic and immunohistochemical features of these tumors, the researchers designated the tumors as a "microcystic stromal tumor" (MCST), which is a novel entity. In their report of 16 cases, the tumors were characterized by the principal microscopic appearance of microcysts, with variably prominent solid cellular areas and fibrous stroma. Diffuse and strong expressions of vimentin and CD10 were also noted. Their precise origin and background genetic alterations remain unclear. However, a stromal nature was favored in the article because of the morphologic resemblance to thecoma and by exclusion of other possibilities.

We recently encountered 2 cases of ovarian MCSTs that exhibited features similar to those reported. In this study, we attempted to further clarify the histologic, immunohistochemical, and genetic features of this unique ovarian neoplasm. We found a previously undescribed "macrocystic pattern" of tumor growth in both MCSTs, along with microcystic and solid patterns. In addition, we recognized a certain degree of morphologic resemblance, particularly in the cellular features, between ovarian MCSTs and pancreatic solid pseudopapillary neoplasms (SPNs). The finding that CD10 and vimentin are both commonly expressed in ovarian MCSTs[7] and pancreatic SPNs[14] was also of interest. These notions have led us to investigate β-catenin alteration in ovarian MCSTs, as pancreatic SPN is well known for harboring a β-catenin mutation.[1,24] Using immunohistochemical analyses, we found that aberrant nuclear accumulation of β-catenin protein occurs in MCSTs. By direct sequencing, we then showed that both tumors harbored an oncogenic somatic mutation in exon 3 of the β-catenin (*CTNNB1*) gene.

Further, we compared the morphology and immunohistochemical profiles of ovarian MCSTs and other

ovarian tumors that can be differentially diagnosed, such as sex cord-stromal tumors, struma ovarii (SO), and yolk sac tumors (YSTs). Among the ovarian tumors, granulosa cell tumor (GCT), along with thecoma, is one of the top differential diagnoses of MCST. By immunohistochemistry we showed that MCSTs do not express sex cord-stromal markers α-inhibin and calretinin, which are frequently positive in GCTs and thecomas. To strictly rule out the possibility that ovarian MCST was a variant of GCT, we also sequenced *FOXL2*, a gene mutated in nearly all ovarian GCTs.[2,8,10,20,21] As neither of the MCSTs harbored the *FOXL2* mutation, we concluded that MCST is a tumor that can be clearly distinguished from the GCT lineage. The ovarian counterpart of pancreatic SPN (ovarian SPN), which was recently reported,[5] is another important entity that requires distinction from MCSTs. As we were unable to identify a case of ovarian SPN, we included pancreatic SPNs in the series of cases assessed for immunophenotypes and attempted to show the difference between MCSTs and SPNs.

To our knowledge, this is the first report describing genetic alterations in MCST. Distinct histologic and immunohistochemical properties of MCST, along with its differential diagnosis, are presented in detail.

MATERIALS AND METHODS

Tissue Samples

We retrieved and reviewed hematoxylin and eosin-stained sections of 2 cases of ovarian MCST. The ovarian tumor in case 1 was surgically removed at the University of Tokyo Hospital, and its pathologic diagnosis was made by 2 of the authors (D.M. and J.S.) on the basis of 17 sections taken from the tumor. Case 2 was from Osaka Rosai Hospital and was retrieved from the consultation files of 1 of the authors (D.M.). Twenty-two slide sections were reviewed for the ovarian tumor in case 2. Neither of the cases was reported previously. The diagnosis of MCST was made on the basis of the criteria proposed by Irving and Young.[7] The tumors were required to exhibit the following features: (1) a microcystic pattern and regions with lobulated cellular masses with intervening, sometimes hyalinized, fibrous stroma, (2) absence of morphologic features enabling any other specific diagnosis in the sex cord-stromal category, (3) absence of epithelial elements, and (4) absence of teratomatous or other germ cell elements. Clinical information was obtained from the clinicians and hospital charts for each case.

In addition, we studied a broad range of ovarian neoplasms that may be included in the differential diagnosis of MCST. The following tumors were retrieved from the archives of the Departments of Pathology of the University of Tokyo and Mitsui Memorial Hospital: 11 adult granulosa cell tumors (AGCTs), 2 juvenile granulosa cell tumors (JGCTs), 11 fibromas, 4 thecomas, 4 fibrothecomas, 2 Sertoli-Leydig cell tumors, 2 stromal tumors with minor sex cord elements, 1 steroid cell tumor, 1 gonadoblastoma, 7 SO, and 8 YSTs. We also retrieved 3 pancreatic SPNs to examine the similarities and differences between ovarian MCSTs and pancreatic SPNs.

Immunohistochemistry

All the tissue samples were fixed in formalin and embedded in paraffin. Full tissue sections (4-μm thick) were used for immunohistochemistry in all cases. Immunohistochemical staining was performed according to standard techniques on a Ventana Benchmark XT autostainer (Ventana Medical Systems Inc., Tucson, AZ). Appropriate positive and negative controls were included. A list of antibodies used in this study and criteria for positive immunoreactivity for each antibody are shown in Table 1.

DNA Extraction and Gene Sequencing of CTNNB1 and FOXL2

We analyzed cases of ovarian MCST for *CTNNB1* and *FOXL2* mutations. Sections (8-μm to 10-μm thick) were cut from paraffin-embedded blocks containing MCSTs and those containing background tubal tissues from the same patients. Representative areas of the sections were macrodissected. Extraction of genomic DNA was performed using a PicoPure DNA Extraction Kit (Life Technologies Corp., Carlsbad, CA). Exon 3 of *CTNNB1*, the gene encoding β-catenin, contains the region involved in glycogen synthase kinase 3β phosphorylation. This exon was amplified using the following primer pairs: F: 5′-GATTTGATGGAGTTGGACATG G-3′ and R: 5′-GCTACTTGTTCTTGAGTGAAGG-3′. A somatic mutation in the *FOXL2* gene was reported to be present in almost all (86 of 89, 97%) morphologically defined AGCTs.[2,8,10,11,20,21] This *FOXL2* c.402C > G mutation changes a highly conserved cysteine residue to a tryptophan (p.C134W). We amplified exon 1 of *FOXL2*, which contains the above mutation, using the following set of primers: F: 5′-CCGCCACAACCTCAGCCTC-3′ and R: 5′-CGCCGGTAGTTGCCCTTCTC-3′. An Applied Biosystems 3730xl DNA Analyzer and 3130xl Genetic Analyzer were used for sequence analysis.

This study was approved by the institutional review boards of the facilities involved.

RESULTS

Clinical Features of Ovarian MCSTs

Case 1

A 33-year-old woman, gravida 0, para 0, with no particular relevant past history was found to have a right ovarian mass and multiple uterine masses. The ovarian mass showed a predominantly solid and partially cystic appearance on a computed tomographic scan, which raised the possibility of a sex cord-stromal tumor. The uterine masses were diagnosed clinically as leiomyomas. The patient initially received a gonadotropin-releasing hormone analog. After treatment, the uterine tumors decreased in size. However, the right ovarian tumor grew larger. Serum lactose dehydrogenase was elevated at 381 IU/L (normal range, 125 to 237 IU/L). Tumor markers, such as carcinoembryonic antigen, CA19-9,

TABLE 1. Antibodies Used for Immunohistochemistry and Criteria for Positive Immunoreactivity

Antibody	Dilution	Clone	Manufacturer	Criteria for Positive Immunoreactivity
CD10	1:200	NCL-CD10-270	Novocastra	Cytoplasmic or membranous staining in > 5% of tumor cells
Vimentin	1:1000	V9	Dako	Cytoplasmic or membranous staining in > 5% of tumor cells
WT-1	1:25	6F-H2	Dako	Nuclear staining in > 50% of tumor cells
β-Catenin	1:2000	14/Beta-Catenin	BD Biosciences	Nuclear staining in > 50% of tumor cells
α-Inhibin	1:50	R1	Dako	Cytoplasmic staining in > 5% of tumor cells
Calretinin	1:25	NCL-Calretinin	Novocastra	Cytoplasmic or membranous staining in > 5% of tumor cells
ER	Prediluted	SP1	Ventana	Nuclear staining in > 50% of tumor cells
PgR	Prediluted	IE2	Ventana	Nuclear staining in > 50% of tumor cells
EMA	1:100	E29	Dako	Membranous staining in > 5% of tumor cells
Cytokeratin (AE1/AE3)	1:100	AE1/AE3	Dako	Cytoplasmic or membranous staining in > 5% of tumor cells
Cytokeratin (Cam 5.2)	Prediluted	Cam 5.2	BD Biosciences	Cytoplasmic or membranous staining in > 5% of tumor cells
Cytokeratin 7	1:100	OV-TL 12/30	Dako	Cytoplasmic or membranous staining in > 5% of tumor cells
CD56	1:50	NCL-CD56-1B6	Novocastra	Membranous staining in > 5% of tumor cells
Synaptophysin	1:100	Poly	Dako	Cytoplasmic staining in > 5% of tumor cells
Chromogranin A	1:200	Poly	Dako	Cytoplasmic staining in > 5% of tumor cells
Desmin	1:100	D33	Dako	Cytoplasmic staining in > 5% of tumor cells
Smooth muscle actin	1:400	1A4	Dako	Cytoplasmic staining in > 5% of tumor cells
CD34	1:20	My10	Becton Dickinson	Cytoplasmic or membranous staining in > 5% of tumor cells
CD31	1:40	JC70A	Dako	Cytoplasmic or membranous staining in > 5% of tumor cells
D2-40	1:60	D2-40	Covance	Cytoplasmic or membranous staining in > 5% of tumor cells
CD99	1:100	12E7	Dako	Membranous staining in > 5% of tumor cells
TTF-1	1:200	8G7G3/1	Dako	Nuclear staining in > 5% of tumor cells
AFP	1:1000	Poly	Dako	Cytoplasmic or membranous staining in > 5% of tumor cells
Ki-67	1:100	MIB-1	Dako	Percentage of tumor cells showing positive nuclear immunoreactivity was calculated as MIB-1 index.

AFP indicates α-fetoprotein; EMA, epithelial membrane antigen; ER, estrogen receptor; PgR, progesterone receptor; TTF-1, thyroid transcription factor 1.

and CA125, were within the respective normal ranges. To make definitive diagnoses of ovarian and uterine tumors, the patient underwent right adnexectomy, enucleation of the uterine masses, and partial omentectomy. The patient is currently free of disease 14 months after surgery.

Case 2

A 41-year-old woman presented with lower abdominal pain. Ultrasonography revealed an ovarian mass. On a computed tomographic scan, the mass was a multilocular cystic lesion that showed mild contrast enhancement. Radiographically, an ovarian mucinous adenocarcinoma was suspected. The patient underwent a right adnexectomy and enucleation of a uterine leiomyoma. The patient is currently free of disease 4 months after surgery.

Gross Features of Ovarian MCSTs

Case 1

The right ovarian tumor measured 11.5 × 6.5 × 5.0-cm. It was confined in the ovary, and the surface of the ovary was smooth. Cut surfaces of the tumor revealed a mixed solid and cystic appearance (Fig. 1A). Solid areas were predominantly whitish. Areas with hemorrhagic change were also observed.

Case 2

The right ovarian tumor weighed 340 g and measured 9.5 cm in maximum diameter. The ovarian surface of the ovary was smooth. Cut surfaces of the tumor revealed a prominent spongy appearance with numerous cystic cavities filled with blood (Fig. 1B). Solid and white areas were also found.

Histologic Features of Ovarian MCSTs

The histologic features of the tumor in case 1 (Fig. 2) and case 2 (Fig. 3) were quite similar. Both tumors were surrounded by fibrous capsules and were well demarcated from the background ovarian parenchyma. A thin layer of ovarian medulla with vascular networks was present on the outer rim of the tumor, and the ovarian cortex was observed circumferentially toward the surface of the ovary. The ovarian cortex was particularly well preserved in the tumor of case 2. Many follicles were observed around the tumor. The principal structural patterns that tumor cells of MCSTs exhibited included a microcystic pattern, a solid pattern, and a macrocystic pattern. The presence of intervening thick fibrous stroma was another feature that characterized MCSTs. The fibrous stroma frequently showed hyalinization. Occasional myxoid change was also seen in the stroma. Areas of hemorrhage with hemosiderin deposition were present within both tumors.

In case 1, solid and microcystic areas predominated, and the macrocystic pattern was seen in a scattered manner. Macrocystic structures were predominant in case 2, and they were easily identifiable on low-power examination. A gradual transition between solid areas, microcystic areas, and macrocystic areas was frequently seen. The tumor occasionally showed a reticular appearance in the areas where irregularly shaped cysts of